Far-infrared absorption by small silver particles in gelatin

R. P. Devaty
Department of Physics and Astronomy, University of Pittsburgh, 100 Allen Hall, Pittsburgh, Pennsylvania 15260

A. J. Sievers
Laboratory of Atomic and Solid State Physics and Materials Science Center, Cornell University, Ithaca, New York 14853-2501

(Received 12 July 1989; revised manuscript received 18 December 1989)

The far-infrared (FIR) properties of a composite material consisting of ~100-Å-diameter silver particles imbedded in a gelatin host are discussed in detail. This material was studied by both transmission electron microscopy—so that the morphology of the particles is well characterized—and FIR spectroscopy. The volume fraction f of Ag is adjustable over a broad range ($0 \le f \le 0.34$). Samples with either well-dispersed or deliberately agglomerated particles were prepared. The procedures for preparation and characterization of this novel composite material are presented. The role of an absorbing host in effective-medium theories of composite materials is examined because gelatin absorbs FIR radiation. The FIR complex dielectric function of gelatin is determined. The Bruggeman model provides agreement with both the frequency and volume-fraction dependences of the absorption coefficient for low-f material ($f \le 0.15$) with well-dispersed particles. The results are used to place bounds on the possible enhancement of the absorption by Ag particles. The Bruggeman model does not describe the data quantitatively for $f > 0.15$. The observed increase in absorption is more gradual than predicted. The Bruggeman model is qualitatively consistent with the low-frequency dielectric constant of the Ag-gelatin composite, which was determined using an interference effect. Samples with deliberately agglomerated particles show enhanced absorption. A simple clustering model predicts enhanced absorption, even though absorption by the gelatin dominates absorption by the Ag particles by at least 2 orders of magnitude for $f = 0.05$.

I. INTRODUCTION

The anomalous enhancement of the far-infrared (FIR) absorption coefficient α of a dilute mixture of ultrafine metal particles (diameter ≤ 100 Å) imbedded in a nonabsorbing host by 1–4 orders of magnitude over the predictions of theory has been of interest since its discovery in 1975 by Tanner *et al.*[1] Further experimental work[2–5] characterized the ubiquity of the enhancement (observed for Al, Ag, Au, Cu, Pd, Sn, and Pt), an approximately quadratic frequency dependence for α, and a linear dependence on metallic volume fraction f for small f [with the exception of Al (Ref. 5)]. However, important information required to distinguish among the many proposed mechanisms[6–16] was lacking. In particular, it is very difficult to determine the morphology of the samples, which were typically pressed pellets of metal smoke prepared by inert-gas evaporation[17] and mixed with an alkali-halide host, by transmission electron microscopy (TEM). There was no convincing experiment to distinguish whether the enhancement is associated with clusters or intrinsic to individual isolated particles.

Progress was made when Devaty and Sievers[18] developed a novel composite material, ~100-Å-diameter Ag particles imbedded in gelatin, which could be examined both by TEM and FIR spectroscopy. Samples with well-dispersed or deliberately agglomerated particles could be produced. Data on this material allowed bounds to be placed on the enhancement for well-dispersed particles. Samples with deliberately agglomerated particles showed enhanced absorption.

Other experiments provided additional evidence associating clustering with enhanced FIR absorption. Curtin *et al.*[19] used heat treatments to modify anomalous behavior of superconducting Sn particles at frequencies near the gap. Lee *et al.*[20] imbedded Ag particles (~900 Å diameter) in du Pont DLX-6000, a Teflon-like material that is a weak absorber in the FIR and, like gelatin, can be ultramicrotomed to prepare samples for the TEM. They found agreement between experiment and theory for well-dispersed particles and observed enhanced absorption for a sample containing clustered particles.

These experiments directed theorists to focus on the role of clustering. A number of models and mechanisms have been proposed, including fused clusters,[21] cluster percolation,[21] clusters of tunnel junctions,[21] self-similarity and fractals,[22,23] and distributions of effective depolarization factors.[24] Mechanisms not based on clustering have also been considered recently, including surface phonons,[25] electron-phonon coupling,[26] diffuse surface scattering,[27] relaxation-time effects,[28] and quantum-size effects.[29]

Recent experiments which focus on details of the FIR absorption such as its temperature dependence[30] and the effect of absorbing oxide coatings on the particles[20,31] can be interpreted within the framework of available theory. A notable exception is the size dependence of the FIR absorption by Al particles.[32] For detailed background the

reader is referred to a number of reviews.[33–37]

This paper presents a detailed study of FIR absorption by small Ag particles imbedded in gelatin. Section II provides theoretical background. Since gelatin absorbs in the far infrared, the effects of an absorbing host on the predictions of effective medium theories are considered. A simple clustering model related to the cluster percolation model of Curtin and Ashcroft[21] is developed. Section III discusses the preparation and characterization of two types of Ag-gelatin composite material. Section IV presents the results of FIR measurements. Data on the volume fraction dependence of α for f up to 0.34 are presented. FIR measurements over such a broad range of f provide a test for theories of inhomogeneous media. Enhanced absorption is observed in low-f samples when the particles are deliberately agglomerated. The volume-fraction dependence of the FIR dielectric constant is obtained from channel spectra. Section V discusses the results. Bounds are placed on the enhancement of α for low-f samples based on several arguments. The Bruggeman model[38] describes the data on well-dispersed particles for $f \leq 0.15$, but breaks down for larger f. Further theoretical work is required to describe FIR absorption by the Ag-gelatin system as f approaches the dc percolation threshold. Section VI summarizes the results on the Ag-gelatin composite, including the disagreement between theory and experiment in the high-concentration limit.

II. THEORY

A. Effective-medium theories

A homogeneous effective frequency-dependent complex dielectric function of a heterogeneous composite material is obtained from an effective-medium theory. Since these theories have been discussed many times,[4,5,33,39] the results are briefly stated here. Landauer[40] has reviewed the history of effective-medium theories.

The electromagnetic absorption coefficient is

$$\alpha(\tilde{\omega})=2\pi\tilde{\omega}\{2[(\overline{\epsilon\mu})_1^2+(\overline{\epsilon\mu})_2^2]^{1/2}-2(\overline{\epsilon\mu})_1\}^{1/2} , \quad (1)$$

where the frequency $\tilde{\omega}$ is expressed in wave numbers (cm^{-1}). The subscripts refer to the real and imaginary parts of a complex quantity according to $z=z_1+iz_2$. $\overline{\epsilon\mu}$ is an effective-medium average of the product of the dielectric function and magnetic permeability. Although Ag particles are nonmagnetic, μ is retained because magnetic dipole absorption is frequently attributed to μ rather than ϵ. The approximation $\overline{\epsilon\mu}\simeq\bar{\epsilon}\bar{\mu}$ is commonly used,[13] although this decomposition must be justified in practice.[41]

The Maxwell-Garnett[42] (MG) effective dielectric function is

$$\bar{\epsilon}=\epsilon_h\frac{(1-f)+3f\epsilon/(2\epsilon_h+\epsilon)}{(1-f)+3f\epsilon_h/(2\epsilon_h+\epsilon)} , \quad (2)$$

where ϵ and ϵ_h are the frequency-dependent complex dielectric functions of the metallic inclusions and host, respectively. The associated microstructural topology is a metal sphere coated with the host.[39]

The Bruggeman[38] (BR) model treats the host and inclusions on an equal basis. The effective dielectric function for a two-component system is obtained by solving the quadratic equation

$$\frac{3f}{2+\epsilon/\bar{\epsilon}}+\frac{3(1-f)}{2+\epsilon_h/\bar{\epsilon}}=1 . \quad (3)$$

This symmetric expression corresponds to a topology of spheres of host and inclusions imbedded self-consistently in the effective medium. The BR model has a dc percolation threshold at $f=\frac{1}{3}$. The BR and MG expressions are equivalent in the limit of vanishing f.

Magnetic dipole absorption must also be included in a treatment of FIR absorption by small metal particles.[1,4,5,43] $\bar{\mu}$ is calculated by replacing ϵ_h and ϵ in the MG and BR models with $\mu_h=1$ and μ, respectively. For a sphere, the magnetic permeability is related to the polarizability per unit volume α_m by[44]

$$\mu=\frac{3+8\pi\alpha_m}{3-4\pi\alpha_m} . \quad (4)$$

For a quasistatic magnetic field[45]

$$\alpha_m=-\frac{3}{8\pi}\left[1-\frac{3}{(ka)^2}+\frac{3}{ka}\cot(ka)\right] , \quad (5)$$

where $k=2\pi\tilde{\omega}(\epsilon\mu)^{1/2}$. In the limit $|ka|\ll 1$, expansion of Eq. (5) leads to

$$\mu\simeq 1+\frac{\pi^2}{10}\epsilon(ka\tilde{\omega})^2 . \quad (6)$$

For small f and low frequencies, the results of an effective-medium treatment reduce to the correct limiting expression obtained from the Mie theory.[46] Equation (6) was used in the calculations discussed in this paper.

The FIR dielectric function of Ag is described by the Drude model. The complex dielectric function $\epsilon=\epsilon_1+i\epsilon_2$ is given by

$$\epsilon=1-\frac{\omega_p^2\tau}{\omega(1-i\omega\tau)} \quad (7)$$

where τ is the electronic relaxation time and ω_p is the bulk plasma frequency. Core polarizability has been neglected. For small Ag particles, the scattering time is determined by boundary scattering.[47] For diffuse scattering $1/\tau=v_F/a$, where v_F is the Fermi velocity and a the particle radius. For Ag,[48] $v_F=1.39\times10^8$ cm/s and $\hbar\omega_p=9.0$ eV.

B. The role of an absorbing host

Since the gelatin host absorbs FIR radiation, it is important to include ϵ_h, the *complex* dielectric function for gelatin, in an effective-medium treatment. For 100-Å-diameter Ag particles in gelatin, $|\epsilon_2|\gg|\epsilon_1|\gg|\epsilon_{h1}|,|\epsilon_{h2}|$. For $|\epsilon_h/\epsilon|\ll 1$ and f sufficiently small, the MG model predicts

$$\bar{\epsilon}_1 \simeq \left[\frac{1+2f}{1-f}\right]\epsilon_{h1} - \frac{18f}{(1-f)^2}\frac{\epsilon_{h1}\epsilon_{h2}}{\epsilon_2} ,$$
$$\bar{\epsilon}_2 \simeq \left[\frac{1+2f}{1-f}\right]\epsilon_{h2} + \frac{9f}{(1-f)^2}\frac{\epsilon_{h1}^2-\epsilon_{h2}^2}{\epsilon_2} . \quad (8)$$

In each equation the first term dominates the second by at least 3 orders of magnitude in the frequency range of interest, for f not too close to 1. Thus,

$$\alpha(\tilde{\omega}) \simeq \left[\frac{1+2f}{1-f}\right]^{1/2} \alpha_{\text{gel}} , \quad (9)$$

where α_{gel} is the absorption coefficient of gelatin. Equation (9) is exact if the Ag particles are treated as perfect conductors.

For the BR model, if $|\epsilon_h/\epsilon| \ll 1$ and $f < \frac{1}{3}$ (but not too close),

$$\bar{\epsilon}_1 \simeq \frac{\epsilon_{h1}}{1-3f} - \frac{18f(1-f)}{(1-3f)^3}\frac{\epsilon_{h1}\epsilon_{h2}}{\epsilon_2} ,$$
$$\bar{\epsilon}_2 \simeq \frac{\epsilon_{h2}}{1-3f} + \frac{9f(1-f)}{(1-3f)^3}\frac{\epsilon_{h1}^2-\epsilon_{h2}^2}{\epsilon_2} . \quad (10)$$

Thus,

$$\alpha(\tilde{\omega}) \simeq \alpha_{\text{gel}}/\sqrt{1-3f} . \quad (11)$$

Equations (9) and (11) demonstrate that in both models absorption by well-dispersed Ag particles is dominated by the gelatin. For sufficiently small f the only effect of the metal particles is the f-dependent coefficient multiplying α_{gel}. The origin of the enhancement is the exclusion of the electric field from the particles.

Equation (11) breaks down as f approaches $\frac{1}{3}$. Figure 1 shows the frequency dependence of α in the BR model for several values of f. Both the electric and magnetic contributions were included. $\mu_h = 1$ was used for gelatin. For all calculations reported in this paper that include absorption by the gelatin, electric dipole absorption (contribution of $\bar{\epsilon}$) dominates magnetic dipole absorption (contribution of $\bar{\mu}$). For $f=0.33$ α is quadratic in frequency for $\tilde{\omega} < 10$ cm^{-1} as for Drude metal particles and unlike the cubic dependence for gelatin. Thus the BR model predicts that absorption by the Ag particles dominates the gelatin absorption below the percolation threshold only as f closely approaches $f = \frac{1}{3}$. For the MG model, the frequency dependence of α does not change over the range $0 \le f \le 0.34$ of interest here.

The absorption coefficient of a composite medium need not be simply related to the absorption coefficients of the constituent materials, especially if both the host and inclusions are absorbers. As a simple example, Fig. 2 shows the volume-fraction dependence of α (based on $\bar{\epsilon}$ only) at 20 cm^{-1} in the BR model for a composite made up of two insulating materials (subscripts A and B) with

$$\epsilon_A = c_{A1} + ic_{A2}\tilde{\omega}^2 ,$$
$$\epsilon_B = c_{B1} + ic_{B2}\tilde{\omega}^2 , \quad (12)$$

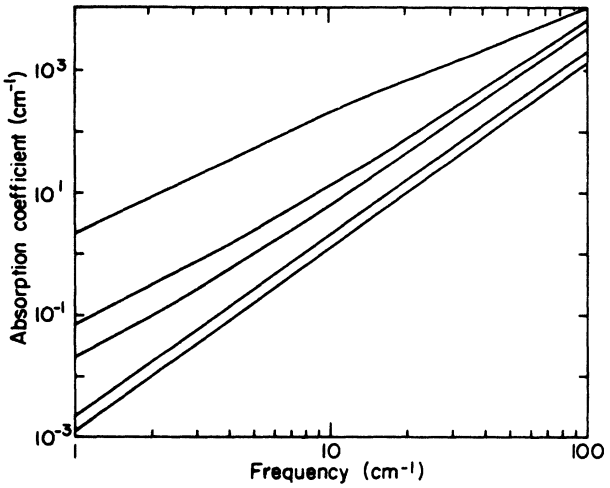

FIG. 1. Frequency dependence of the FIR absorption coefficient of 100-Å-diameter Drude Ag particles in gelatin according to the Bruggeman model. The curves, in ascending order, correspond to $f=0.0$, 0.20, 0.31, 0.32, and 0.33. The dielectric function for gelatin is $\epsilon_h = 3.3 + i3.61\times10^{-4}\tilde{\omega}^2$.

where the c's are constants. ϵ_A and ϵ_B have the same form as the model for gelatin. For certain combinations of the c's, α can be significantly enhanced with respect to the values for each constituent.

C. Clustering effects

This work[18] and other recent experiments[19,20] demonstrate that clustering of the particles is associated with an

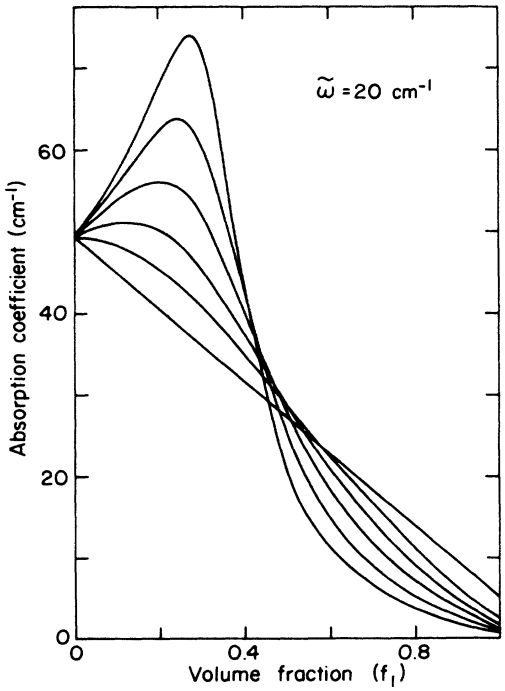

FIG. 2. Volume-fraction dependence of the absorption coefficient at $\tilde{\omega}=20$ cm^{-1} predicted by the Bruggeman model for a two-component system with dielectric functions $\epsilon_A = c_{A1} + i1.0\times10^{-4}\tilde{\omega}^2$ and $\epsilon_B = 1.0 + i1.0\times10^{-3}\tilde{\omega}^2$. The curves correspond to $c_{A1}=1$, 5, 10, 20, 40, and 80, in order of increasing absorption at $f_A = 0.2$.

enhancement of the FIR absorption coefficient. Curtin and Ashcroft[21] introduced three models which show how clusters of particles lead to enhanced absorption. The cluster percolation model, which applies to electrically isolated particles, is the most appropriate for application to the Ag-gelatin composite. The low electrical conductivity of a cluster with f near the dc percolation threshold produces the enhancement. The origin of the enhancement can be regarded as a resonance in the volume-fraction dependence of the absorption by a cluster, in analogy with the plasma-sphere resonance in the frequency dependence of α for isolated small particles. Curtin and Ashcroft[21] used the real-space renormalization group to model clusters. A simple model which produces a similar effect is described here.

A cluster of particles is replaced by an homogeneous sphere made up of an effective medium with dielectric function $\epsilon_c(\tilde{\omega};p)$. The BR model is chosen because it has the percolation properties required to produce the enhancement. An actual sample will contain a distribution of clusters covering a range of metallic volume fractions, with perhaps only a small fraction near percolation. Assume that the details of the cluster distribution are unimportant. Consider a distribution which is ur - form over a range of volume fractions p that includes the percolation threshold p_c. The cluster distribution $P(p)$ is defined so that $P(p)dp$ is the probability that a cluster has a metallic volume fraction between p and $p+dp$. Note that

$$\int_0^1 P(p)dp = 1 \ . \tag{13}$$

Choose the upper limit of the uniform distribution as $p_m = 0.7$, which is approximately the value for close packing of spheres. The lower limit is $p=0$. Assume $f \ll 1$, where f is the volume fraction of metal in the sample.

The effective dielectric function of the medium of clusters imbedded in a gelatin host can be obtained using the multicomponent MG model:[39]

$$\bar{\epsilon} = \epsilon_h(\tilde{\omega}) \frac{(1-f') + 3f' \int_0^1 \frac{\epsilon_c(\tilde{\omega};p)P(p)}{2\epsilon_h(\tilde{\omega}) + \epsilon_c(\tilde{\omega};p)} dp}{(1-f') + 3f' \int_0^1 \frac{\epsilon_h(\tilde{\omega})P(p)}{2\epsilon_h(\tilde{\omega}) + \epsilon_c(\tilde{\omega};p)} dp} \ . \tag{14}$$

Here $f' \equiv f/\bar{p}$, where $\bar{p}$ is the mean of p. Note that effective-medium theory has been applied twice: first the BR model to treat the clustering, then the MG model to treat the entire sample.

III. EXPERIMENT

Progress in understanding the physics of small particles depends largely upon advances in techniques for sample preparation. To examine the role of clustering in the anomalous FIR absorption, it is desirable to examine the same material as used in the spectroscopic measurements with a transmission electron microscope (TEM). Samples with particles imbedded in an alkali halide, an excellent host for FIR studies, are unsuitable for examination in a TEM. Unsupported metal particles, such as those prepared by inert-gas evaporation,[17] are easy to study with the TEM, but they are clumped and perhaps coated with an absorbing oxide as well.

An ideal metal-insulator composite material for FIR studies would have the following characteristics: (1) adjustable metallic volume fraction, to test effective-medium theories, (2) monodisperse particles with adjustable size, to simplify the analysis and to facilitate searches for quantum-size effects, (3) a transparent dielectric host, (4) the ability to control clustering, and (5) the ability to produce the material in sufficient quantities (grams). The requirements for a TEM study are: (1) thin samples (<1000 Å thick), (2) good image contrast between the particles and the supporting host, (3) a host that is insensitive to beam damage, and (4) a host with good thermal conductivity to minimize heating of the sample by the electron beam. No composite material with all of these properties has been produced. Progress depends on developing a compromise that retains the properties required to address at least some of the unanswered questions.

The material of concern in this paper is roughly 100-Å-diameter Ag particles supported by gelatin. This material can be examined in the TEM. Samples with either well-dispersed or deliberately clustered particles can be prepared. The volume fraction of Ag is adjustable over a broad range. The principle drawback of this material is that the gelatin absorbs FIR radiation, which masks absorption by the particles for small f.

A. Sample preparation

This section describes the procedure for preparing the Ag-gelatin composite material. The Ag particles are obtained as a colloidal suspension in water by reduction of $AgNO_3$ according to the method of Carey Lea.[49] This hydrosol has also attracted interest in studies of surface-enhanced Raman scattering.[50] Use of a sol eliminates the need to disperse the particles in a medium, as they are prepared in a suspended dispersed form. The Carey Lea sol was chosen because the concentration of Ag particles is orders of magnitude higher than the yield for other recipes.

1. Carey Lea sol

The recipe for Carey sol is described in detail by Frens and Overbeek.[51] Typically, 200 ml of sol were prepared at a time. Twice distilled (2×) water was generally used. The reducing agent, dissolved $FeSO_4$ and sodium citrate, was stirred magnetically. A solution of dissolved $AgNO_3$ was quickly poured in. The solution immediately turned brown as the Ag ions were reduced to neutral Ag, which condensed to form Ag particles. The particles agglomerated due to the high concentration of ions and precipitated to the bottom of the beaker. The sol was centrifuged and the supernatant discarded. A washing cycle consisting of resuspending the particles in water (repeptization), followed by reflocculation using sodium citrate and centrifugation, was repeated three times. The particles were resuspended in distilled water to obtain the sol.

It was dark brown in appearance. When diluted sufficiently, it was yellow.

The properties of Carey Lea sol were thoroughly investigated by Frens and Overbeek.[51] For their preparations, the mean particle diameters ranged from 74 to 90 Å as determined by TEM. X-ray analysis revealed that the particles have the normal Ag lattice. There is evidence for a monolayer of adsorbed citrate on the Ag particles based on chemical analysis.[52] The citrate monolayer is apparently responsible for the stability of the sol. As it desorbs over time, the particles tend to agglomerate. Miller and Henz[53] claim that this flocculation is accelerated by light.

2. *Use of gelatin*

It is well known that addition of gelatin stabilizes a hydrosol.[54] The gelatin coats the particles and sterically prevents aggregation. In this work, the gelatin is used to support the Ag particles after the water is removed.

Gelatin was weighed out and dissolved in 2× water in a beaker that was warmed by running hot tap water over the outside. After the Carey Lea sol was added, the beaker was kept warm by placing it in a larger beaker of hot tap water. The solution was stirred occasionally over a period of half an hour.

The gelatin was polymerized in order to obtain thin sections with the ultramicrotome. Otherwise, the gelatin would soak up water as it was being cut and the sections would be destroyed. The gelatin was crosslinked with 25% glutaraldehyde. First, glutaraldehyde was added to give a final concentration of one–two percent by volume in the solution. The sol was allowed to stand for about an hour. If the intended volume fraction of Ag in the final composite material is high, the concentration of gelatin is low, and the solution remains liquid. When there is more gelatin (low f), crosslinking leads to a rubbery mass.

Two methods were used to remove the water: acetone drying (AD) and freeze drying (FD). Acetone was added to the polymerized sol in steps until the water was entirely replaced. The material contracted slowly and became black and brittle as the concentration of acetone was increased. For high-f material, the samples were centrifuged after the acetone concentration was brought to 70% and after each subsequent step of dehydration. After centrifugation, the supernatant was discarded and more acetone added. After standing overnight, the acetone was discarded and the material was dried in air for a few hours. The remaining acetone was removed by pumping in a dessicator. The result was a brittle black powder. The powder was sometimes ground with a mortar and pestle before pressing pellets to improve homogeneity.

Freeze drying was accomplished using a commerical lyophilizer. First the material was poured into a 1200-ml freeze-dry flask and frozen in liquid nitrogen. The material was frozen against the sides of the flask to maximize the surface area exposed to the vacuum. The material was lyophilized for at least 24 h. The resulting material was fluffy and much different in appearance than AD material. For low f, the material picked up static charges easily. Thus it was difficult to handle. Low-f material was brown, whereas material with more Ag was grey. Some samples that were treated with sodium citrate or $NaNO_3$ had a greenish hue. Some samples with deliberately agglomerated particles contained black specks and were clearly inhomogeneous.

Addition of monovalent ions to colloidal hydrosols induces flocculation.[51] Two salts—sodium citrate and sodium nitrate—were used to induce clumping to ensure that the observed effects were not peculiar to a particular salt. Three series of samples, called K, L, and M, were prepared. For each series, five portions of Carey Lea sol taken from the same batch were used. When the desired amount of salt was added to each portion, the sol took on a muddy appearance and the particles precipitated out. For series K and L, sodium citrate was used, whereas the clumping agent for series M was $NaNO_3$. After the portions were stirred, gelatin was added and the material was freeze dried.. Since the salts are nonvolatile, they remain in the dried material. Samples of gelatin and salt with the Ag sol replaced by water were also prepared to test the effect of the salts on the FIR absorption.

3. *Epon imbedding and ultramicrotomy*

To make thin sections suitable for the TEM it is necessary to imbed the Ag-gelatin material in an epoxy for support. This procedure is used by biologists to obtain sections of cells. The material must be dehydrated before infiltration with epoxy. After the epoxy is cured, sections are cut with an ultramicrotome. The epoxy used here, Epon 812, is a popular choice. Other procedures are discussed by Hayat.[55]

It is important that the epoxy thoroughly infiltrate the gelatin to obtain good sections. Infiltration is accomplished by soaking the sample in epoxy for an extended period of time before curing. Small pieces of the material were soaked in acetone prior to infiltration. The acetone is replaced by epoxy in the following steps: 1:3 epoxy:acetone, $\frac{1}{2}$ h; 1:1, 1–2 h; 3:1, overnight to two days; and epoxy only (twice), 1–2 h. During infiltration the epoxy is slowly agitated by turning the vials at a few rpm on a rotor.

After imbedding, pieces of sample were transferred to the bottom of standard molds for ultramicrotomy, which were then filled with epoxy. The samples were cured at 70 °C for a day or two.

Sectioning was done using a du Pont Sorvall MT-2 ultramicrotome with a diamond knife. The sections were about 500 Å thick.

4. *Pressed pellets*

Samples for FIR studies were prepared by pressing at 9–10 tons on a 13-mm-diameter commercial "KBr" die. The die was pumped for 10 min before pressing. The pellets were stored in a dessicator, since gelatin is hygroscopic.

Pellets with low-f AD material resembled little hockey pucks. Pellets made from low-f FD material were dark brown and macroscopically inhomogeneous due to difficulty in working with the material. Pellets of FD gelatin without Ag were also nonuniform. High-f pellets

($0.25 \leq f \leq 0.34$) appeared shiny and metallic for both types of material. The AD material is clearly superior for the production of uniform pressed pellets.

B. Sample characterization

1. Metallic volume fraction

Three methods were used to determine the volume fraction of Ag in the composite material: potentiometric titration, atomic-absorption spectroscopy, and neutron-activation analysis. The quantity that is actually determined by these techniques is the weight fraction of Ag f_W. The volume fraction is obtained from $f = Mf_W/(\rho_{Ag}V)$, where M is the mass of the sample of volume V and ρ_{Ag} is the density of Ag [$\rho_{Ag} = 10.5$ g/cm^3 for bulk Ag (Ref. 56)]. After careful consideration, potentiometric titration (PT) was chosen as the most reliable method. The results using the other two techniques are discussed elsewhere.[57]

The use of PT to determine the concentration of Ag ions in solution is a standard undergraduate experiment in chemistry.[58-59] The potential of a Ag indicator electrode with respect to a saturated calomel reference electrode (SCE) is monitored. As measured amounts of NaCl solution of known concentration are added from a buret, the Cl^- combines with the Ag^+ to form AgCl, a sparingly soluble salt that precipitates out. The accuracy of this technique depends on the rapid change of potential near the equivalence point. The solubility product of the precipitate should be chosen as low as possible[60] to obtain the largest change in potential from beginning to end. In retrospect, AgI ($K_{sp} = 8.49 \times 10^{-17}$) is preferable to AgCl ($K_{sp} = 1.76 \times 10^{-10}$).[61]

Two methods were used to dissolve the Ag particles prior to titration. For dry samples, about 20 drops of 70% (by weight) HNO_3 and a roughly equal amount of 2× water were used. Afterwards, about 50 ml of 2× water were added. The crosslinked gelatin in AD material would not dissolve completely. For the second method, 50 drops of dilute (1%) H_2SO_4 and 50 drops of 30% H_2O_2 were added to 2 ml of Carey Lea sol. About 50 ml of 2× water were added afterwards.

Table I shows the results of PT's. When a titration was repeated, the second value of f_W was always a bit higher. This result was expected because titrations were repeated when undissolved Ag was observed. More care was taken to completely dissolve the Ag the second time.

The accuracy of PT was tested by performing titrations on samples of $AgNO_3$ with known concentration. The presence of gelatin, crosslinked gelatin, and/or nitric acid did not influence the result. However, when one drop of 5N NaOH was added to some dissolved $AgNO_3$, a brown precipitate was formed. Thus, an acidic solution is required. The conclusions are that the reproducibility of PT is better than ±0.3% and the accuracy is better than 5%. The accuracy might be much better because the error measured in the tests might be systematic. The $AgNO_3$ was measured out in a graduated cylinder which is only accurate to ±5%.

2. Transmission electron microscopy

Two instruments were used. A JEM 200 was calibrated by taking micrographs of a Ladd Research Industries, Inc., "waffle" carbon replica of a diffraction grating for a series of magnifications. Later work was performed on a JEOL 200CX TEMSCAN, for which the indicated magnifications were assumed correct. The microscopes were used at their maximum operating voltages, 200 kV.

Samples of Carey Lea sol dried on carbon-coated Cu grids were examined. Figure 3 shows a micrograph of such a sample. It was prepared by diluting some Carey Lea sol by a factor of 10 with water, placing a droplet on a glass microscope slide, putting a bowed Cu grid on the droplet, and allowing the sol to dry. The contrast is excellent and the image is sharp because the particles are unsupported. However, there is no information on the configuration of the particles in the original sol. This micrograph is atypical for dried sol because it shows a large number of isolated particles. Usually, no matter how small the droplets were made, including spraying a grid with a mist of sol using a nebulizer, the particles clumped up when dried. Electron diffraction on samples of dried sol shows that the particles have the fcc lattice of bulk Ag. An accurate determination of the lattice constant

TABLE I. Properties of Ag-gelatin composite materials. AD=acetone dried, FD=freeze dried, C=clumped by addition of a monovalent salt, σ_f=standard deviation of f about the mean.

Material	Preparation method	f_W	f	σ_f
A	AD	0.175	0.025	0.0002
B	AD	0.564	0.142	0.002
C	AD	0.600	0.154	0.007
D	AD	0.457	0.095	0.001
E	FD	0.469	0.121	0.004
F	FD	0.486	0.116	0.002
G	FD	0.593	0.197	0.002
H-1	FD	0.359	0.062	0.0047
I	FD	0.621	0.219	0.006
J	FD	0.605	0.244	0.007
K-1	FD	0.256	0.035	0.0026
K-2	FD,*C*	0.0723	0.012	0.0003
K-3	FD,*C*	0.143	0.0235	0.0007
K-4	FD,*C*	0.0993	0.0165	0.0005
K-5	FD,*C*	0.228	0.035	0.0012
L-1	FD	0.357	0.0585	0.0042
L-2	FD,*C*	0.0641	0.011	0.0001
L-3	FD,*C*	0.171	0.030	0.0004
L-4	FD,*C*	0.220	0.038	0.0013
L-5	FD,*C*	0.119	0.022	0.0002
M-1	FD	0.340	0.059	0.0016
M-2	FD,*C*	0.199	0.039	0.0011
M-3	FD,*C*	0.240	0.045	0.0012
M-4	FD,*C*	0.281	0.051	0.0017
M-5	FD,*C*	0.307	0.056	0.0021
N	AD	0.748	0.310	0.005
O	AD	0.752	0.340	0.009
P-1	AD	0.588	0.161	0.001
P-2	AD	0.689	0.253	0.002

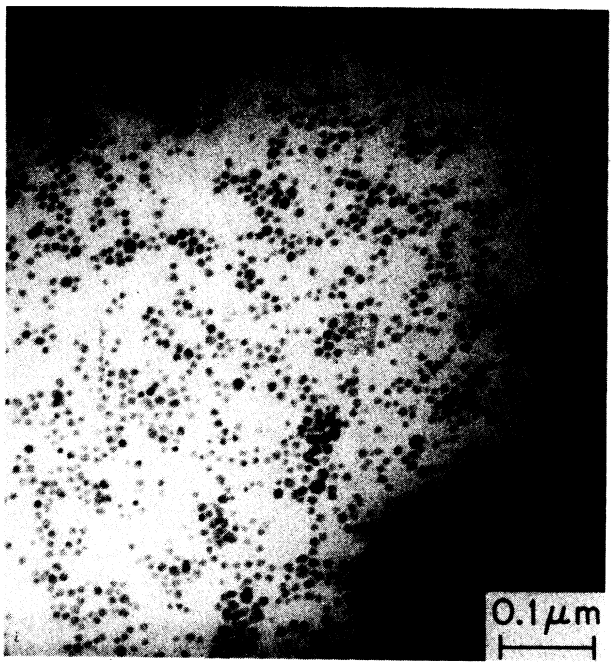

FIG. 3. Transmission electron micrograph of dried Carey Lea sol taken with the JEM 200.

was not possible. The lattice constant of small particles can differ from the bulk.[62]

An attempt was made to examine Carey Lea sol itself in the TEM using a closed wet cell[63] purchased from E. F. Fullam, Inc. The particles moved around and coalesced under electron irradiation, so no significant results were obtained. Observation of the particles was difficult because the films covering the grids in the cell were so thick.

Figure 4 shows selected electron micrographs of Ag-gelatin composite material. Micrographs of low-f material are the most informative. Figure 4(a) shows material A. The particles are generally well dispersed, but there are a few clusters. It is not possible to determine whether overlapping particles are touching due to the lack of depth resolution. Figures 4(b) and 4(c) show AD material with large volume fractions of Ag. There are increasing numbers of larger particles. Some of the large stuff may be the result of beam damage. For samples with closely spaced particles, the image would change in appearance when first irradiated with the beam. At times, particles appeared to melt and coalesce, evaporate, or fly off the sample. Frens and Overbeek[51] also observed coalescence of Ag particles under electron irradiation. The melting temperature of small metal particles tends to be reduced with respect to the bulk.[64,65] Figure 4(c) shows holes in the gelatin and/or Epon where particles were blown away by the beam. Beam damage might be reduced by evaporating carbon onto the sample.

Selected-area electron-diffraction patterns for AD Ag-gelatin composite are complex. There are numerous rings, some of which are associated with Ag. The remaining rings could not be identified. The most likely candidate, sodium citrate, does not have the observed pattern.

The conclusion of analysis by TEM is that AD Ag-gelatin composite is a random conglomerate of small Ag particles of approximately uniform size (at least for small f) supported by the gelatin matrix.

Macroscopically, the freeze-dried material was quite different in appearance from the acetone-dried material. When viewed in the TEM, the differences aren't as apparent. Figure 4(d)–4(f) shows a sequence of micrographs of the FD material in order of increasing f. The particles in low-f material are well dispersed. As f increases, the micrographs show increasingly dense but homogeneous mats of particles. In Fig. 4(f) the particles appear to be clustered rather than uniformly distributed. This effect could be the result of the process of imbedding and slicing material containing so much Ag. Also, the particles shown in Fig. 4(f) are larger than those in Fig. 4(d).

Electron-diffraction patterns of FD material show intense Ag rings but only weak rings and/or spots associated with other substances, in contrast with the AD material. This result is contrary to expectation. When a sample is freeze dried, whatever is nonvolatile in the sample remains there, whereas some components (e.g., sodium citrate) might be lost when the acetone is changed.

Electron microscopy was performed on the series of samples containing particles that were deliberately agglomerated. Micrographs which compare well dispersed and agglomerated particles have been published.[18]

It is possible to determine the particle size distribution for samples with sufficiently low f that the micrographs show nonoverlapping particles. Figure 5 shows the size distribution for material A. A thorough study of the size distribution was not undertaken because the details of the distribution are not thought to be important to the mechanism for the enhanced FIR absorption. The mean particle diameter was typically about 100 Å. No attempt was made to vary the particle size. Note the bimodal nature of the size distribution, which shows a relatively large number of very small particles. This distribution is certainly not well described by the log-normal curve that applies to inert-gas evaporated particles.[17]

C. Far infrared measurements

The FIR absorption coefficient of pressed pellets of Ag-gelatin composite material was measured using Fourier-transform spectroscopy. A lamellar grating interferometer[66] produced modulated radiation over the range 2–70 cm^{-1}. Two cryostats were used. The first[67] has a 2.5-in.-diameter sample chamber that can accept inserts containing up to five samples of about 0.5 in. diameter. The samples were usually immersed in liquid ^4He ($T=4.2$ K). The cryostat contains a charcoal-pumped ^3He refrigerator to cool the Ge bolometer.[68] Plexiglass[69] and black polyethylene filters were used. A second cryostat[70] was used for studies of temperature and/or magnetic field dependence. It contains a 75-kG superconducting solenoid. Because the bore of the magnet is narrow, only one sample could be studied at a time. The bolometer in this system is cooled by an external ^3He system with a Hg diffusion pump.

The frequency-dependent absorption coefficient is determined using

$$\alpha(\tilde{\omega}) = -\frac{1}{\Delta d}\ln\left|\frac{I_2(\tilde{\omega})}{I_1(\tilde{\omega})}\right| . \quad (15)$$

$I_1(\tilde{\omega})$ and $I_2(\tilde{\omega})$ are the Fourier transforms of the interferograms measured for two samples of thicknesses d_1 and d_2, respectively, and $\Delta d = d_2 - d_1$.

There are a number of reasons why the measured α might differ from the true α. If the samples have flat

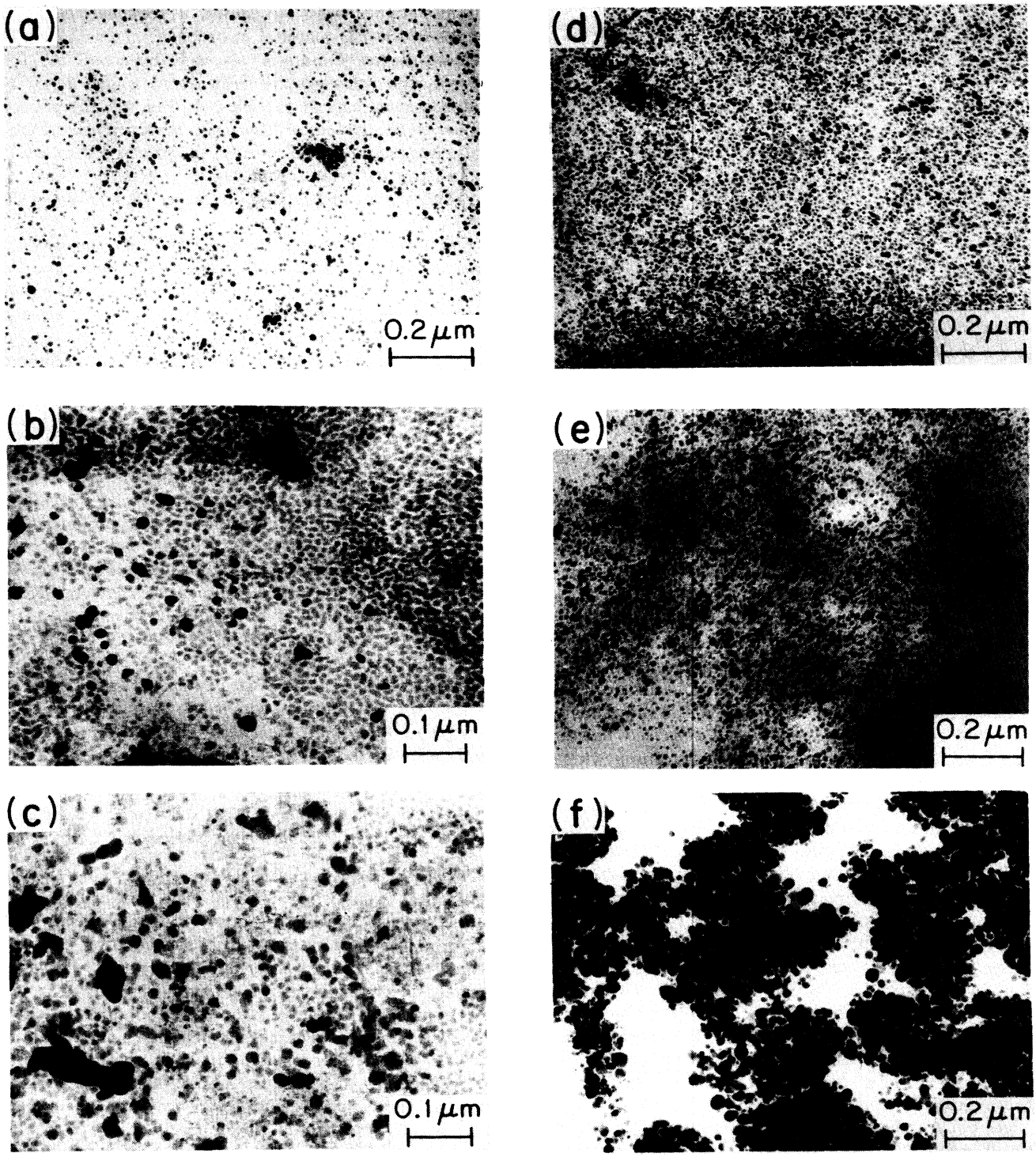

FIG. 4. Transmission electron micrographs of Ag imbedded in gelatin: (a) Material *A*, (b) *P*-1, (c) *O*, (d) *H*-1, (e) *F*, (f) *J*. (a)–(c) shows AD material, (d)–(f) FD. The lower micrographs correspond to higher f. Micrographs (b) and (c) were taken with the JEOL 200CX, the remainder with the JEM 200.

parallel faces, α will be modulated by oscillations due to interference between waves that have undergone multiple reflections. For a plane wave at normal incidence, the transmission is[71]

$$T(\tilde{\omega})=\frac{I_t}{I_i}=\frac{(1-R)^2(1+n_1^2/n_2^2)e^{-\alpha d}}{(1-Re^{-\alpha d})^2+4e^{-\alpha d}\sin^2(\delta+\phi)}\ , \tag{16}$$

where I_i and I_t are the incident and transmitted intensities, d is the thickness of the sample, R the reflectivity, $\delta=2\pi n_1\tilde{\omega}d$, $n=n_1+in_2$ is the complex index of refraction, and

$$\phi=\tan^{-1}\left[\frac{2n_2}{n_1^2-1+n_2^2}\right]\ . \tag{17}$$

Thus, the measured absorption coefficient is

$$\alpha_{\text{meas}}=-\frac{1}{\Delta d}\ln\left|\frac{T_2}{T_1}\right|=\alpha-\frac{1}{\Delta d}\ln\left|\frac{(1-Re^{-\alpha d_1})^2+4Re^{-\alpha d_1}\sin^2(\delta_1+\phi)}{(1-Re^{-\alpha d_2})^2+4Re^{-\alpha d_2}\sin^2(\delta_2+\phi)}\right|\ , \tag{18}$$

where α is the true absorption coefficient. Figure 6 shows the measured absorption coefficient for material P-1 and the predictions of Eq. (18).

α_{meas} can also differ from the true α because the sample positions in the rotator are inequivalent and/or the detector is nonlinear.[72] Both of these factors produce small vertical displacements of $\alpha(\tilde{\omega})$ that can easily be corrected, since $\alpha(\tilde{\omega})$ tends to zero as $\omega\rightarrow 0$. However, for the samples with the highest f, particularly for material O, $\alpha(\tilde{\omega})$ did not reproduce well from sample to sample, and it was difficult to extrapolate α to zero frequency. The variation of the detector resistance from sample to sample was small. An attempt was made to measure α over a narrow bandwidth of low frequencies using thicker samples. For a narrow bandwidth the value of α at the center frequency can be estimated without a Fourier transform by using the white-light signals (measured intensities with the interferometer set to zero path difference) for two samples. Once again the zero-frequency intercepts of $\alpha(\tilde{\omega})$ were not obvious. Also, the measured α's differed for various combinations of pellets of the same material. It is possible that pressed pellets of a given material have different α's for different thicknesses. Densities for material O ranged from 4.52 to 4.95 g/cm^3. Thinner pellets were less dense. Thus, f can vary by a couple percent from sample to sample. Ignoring interference, if the α's are different,

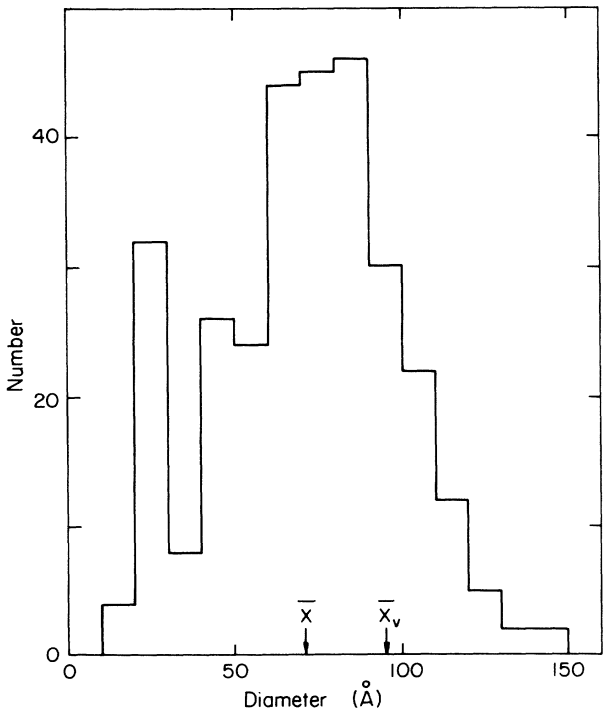

FIG. 5. Size distribution for material A. $\bar{x}$ and $\bar{x}_v$ are the mean diameter and volume-weighted mean diameter, respectively.

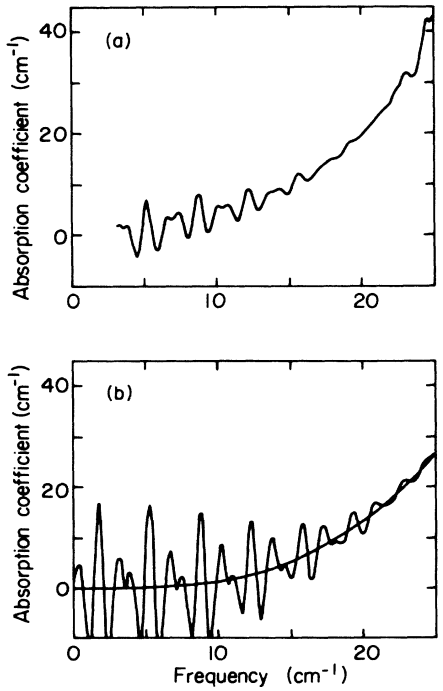

FIG. 6. Absorption coefficient for material P-1. (a) Data, (b) prediction using Bruggeman model both with and without interference due to multiple reflections. The dielectric function for gelatin is $\epsilon_h=3.3+i3.61\times10^{-4}\tilde{\omega}^2$. Also, $d_1=0.106$ cm, $d_2=0.156$ cm, and $n_1=2.71$.

$$\alpha_{\text{meas}}=\frac{\alpha_2 d_2-\alpha_1 d_1}{\Delta d}-\frac{2}{\Delta d}\ln\left|\frac{1-R_2}{1-R_1}\right| + \frac{1}{\Delta d}\ln\left|\frac{1-R_1^2 e^{-2\alpha_1 d_1}}{1-R_2^2 e^{-2\alpha_2 d_2}}\right| . \quad (19)$$

The first term states that α_{meas} is a linear combination of α_1 and α_2. The second term leads to a shift of α_{meas} if $R_1 \neq R_2$, even at zero frequency. Since these difficulties were not resolved, the α's reported below are averages over combinations of samples.

IV. RESULTS

A. Far-infrared properties of gelatin

Figure 7 shows the measured absorption coefficient for acetone-dried gelatin. A smooth curve was drawn through the Fabry-Perot oscillations and the data were shifted so that $\alpha(\tilde{\omega}=0)=0$. The data are well approximated by a cubic frequency dependence. The dielectric function

$$\epsilon_h=\epsilon_{h1}+iC\tilde{\omega}^2 , \quad (20)$$

where ϵ_{h1} and C are real constants, leads to a cubic power law for α if $C\tilde{\omega}^2 \ll \epsilon_{h1}$, which holds over the frequency range of interest.

ϵ_{h1} was determined by taking advantage of multiple internal reflections. A signature of multiple reflections is a secondary maximum (quasi-white light) in the interferogram with the moving mirror displaced a distance $x=nd$ with respect to the position of zero path difference. n is the index of refraction of the sample and d its thickness. Pellets of FD gelatin did not exhibit "secondary interferograms," so only interferograms for AD gelatin were analyzed. For 12 interferograms, $n=1.82\pm0.03$ or $\epsilon_{h1}=n^2=3.30\pm0.10$, where the uncertainty is the standard deviation about the mean. For two pellets of pressed gelatin as taken from the bottle, $n=1.76\pm0.04$ and $\epsilon_{h1}=3.10\pm0.15$.

Given ϵ_{h1}, the equation

$$\alpha_{\text{gel}}=2\pi\tilde{\omega}[2(\epsilon_{h1}^2+\epsilon_{h2}^2)^{1/2}-2\epsilon_{h1}]^{1/2} \quad (21)$$

can be inverted to give

$$\epsilon_{h2}=A(A^2+2\epsilon_{h1})^{1/2} , \quad (22)$$

where $A=\alpha/(2\sqrt{2}\pi\tilde{\omega})$. Figure 8 shows the frequency dependence of ϵ_{h2} for the data shown in Fig. 7. The agreement with a quadratic power law is good. From an average of three measurements, $C=(3.61\pm0.17)\times10^{-4}$ cm^2. The material used for these pellets was prepared at the same time as materials $N-P$. For older acetone-dried gelatin ($A-D$), $C=(4.73\pm0.68)\times10^{-4}$ cm^2 for an average over seven measurements. For FD gelatin, $C=(2.89\pm0.24)\times10^{-4}$ cm^2 for six measurements. Two runs on pressed gelatin straight from the bottle gave $C=(3.60\pm0.02)\times10^{-4}$ cm^2. Note that $\epsilon_{h1}=3.3$ was used in all cases.

B. FIR absorption by Ag-gelatin composite material

1. Frequency dependence

Figures 9–12 show the measured frequency dependence of the FIR absorption coefficient of AD Ag-gelatin composites over a range of Ag volume fractions up to

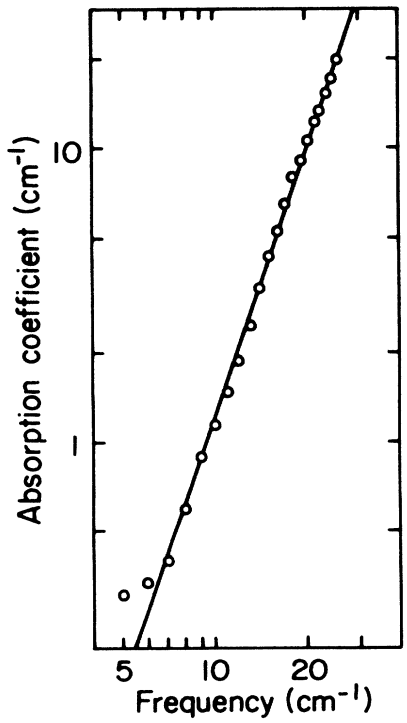

FIG. 7. Absorption coefficient of AD gelatin. The circles represent the data and the line indicates a cubic power law.

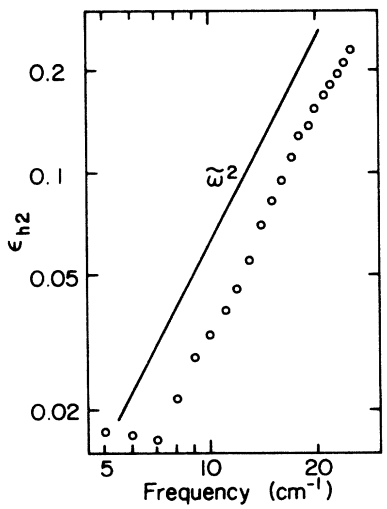

FIG. 8. Frequency dependence of the imaginary part of the dielectric function of AD gelatin. The circles represent the data. The line is a guide to the eye indicating a quadratic power law.

$f=0.34$. Also shown are the predictions of the Bruggeman model using the complex dielectric functions of gelatin (measured) and Drude Ag. Both the electric and magnetic dipole terms are included, although the contribution of the magnetic dipole term is negligible. Theory and experiment agree in both magnitude and frequency dependence to within the uncertainty in the gelatin absorption for $f<0.15$. In this region, absorption by the gelatin dominates and the observed dependence on f is associated with field exclusion [Eq. (11)]. For $f>0.15$, the measured α exceeds the prediction, although not by orders of magnitude, and the frequency dependence is weaker. Note that none of the data shown in these figures has been shifted vertically. A deviation of the frequency dependence from the cubic dependence of gelatin is evidence that absorption by the Ag particles makes an important contribution at lower f than predicted by the BR model.

Figure 9 shows results for materials A and D. The measured α lies between the predicted curves using the dielectric functions of "old" and "new" AD gelatin. For materials $A-D$ the "old" gelatin is appropriate, so the measured absorption is actually less than the theoretical prediction. Figures 10 and 11 show results for samples with f near 0.15. Experiment is slightly greater than theory for all three materials. Agreement can be achieved for material C by downshifting the data by 0.7 cm^{-1}. The low-resolution data at low frequencies indicate a positive intercept, so such a shift is justified. The frequency dependence predicted by the BR model agrees with the data. Figure 11(b) shows a significant enhancement of experiment over theory for material P-2 and a frequency dependence that is closer to linear than cubic. Figure 12 displays results for materials N and O. The measured frequency dependence is weaker than linear, although the large oscillations preclude accurate identification of the baseline. Absorption by the Ag particles dominates. For material O, curves for the BR model are not shown because the model predicts that α blows up at $f=\frac{1}{3}$. However, the frequency dependence shown in Fig. 12(b) resembles that for the Drude model when $\omega\tau \ll 1$, i.e.,

$$\alpha(\tilde{\omega})=4\pi\sqrt{\sigma_0\tilde{\omega}/c}\ , \tag{23}$$

where σ_0 is the dc conductivity of material O, and c the speed of light. The resistivity at 4.2 K obtained from fitting the data is 4.4×10^5 $\mu\Omega$ cm. The room-temperature resistivity of pressed pellets of material O, measured by four-point probe, ranged from 3.5×10^5 to 8.0×10^5 $\mu\Omega$ cm. If the Drude model for a bulk metal provides the correct description of material O, the Ag particles must be strongly coupled.

The data for AD Ag-gelatin composites indicate a gra-

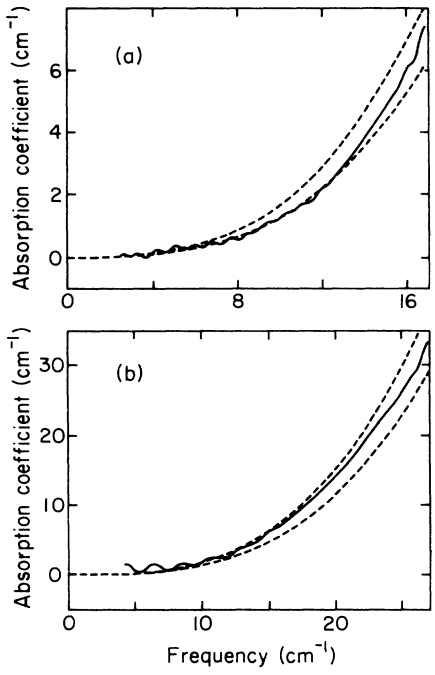

FIG. 9. Frequency dependence of the absorption coefficient of AD Ag in gelatin. (a) Material A, $f=0.025$, resolution 0.62 cm^{-1}. (b) Material D, $f=0.095$, resolution 0.99 cm^{-1}. The solid curves indicate the data. The dashed curves show the predictions of the Bruggeman model for 100-Å-diameter Drude Ag particles in gelatin using the dielectric functions $\epsilon_h=3.3+$ $+i4.73\times10^{-4}\tilde{\omega}^2$ (upper) and $\epsilon_h=3.3+i3.61\times10^{-4}\tilde{\omega}^2$ (lower) for gelatin. Note that the scales of the graphs in (a) and (b) are not the same. This comment also applies to Figs. 10–15.

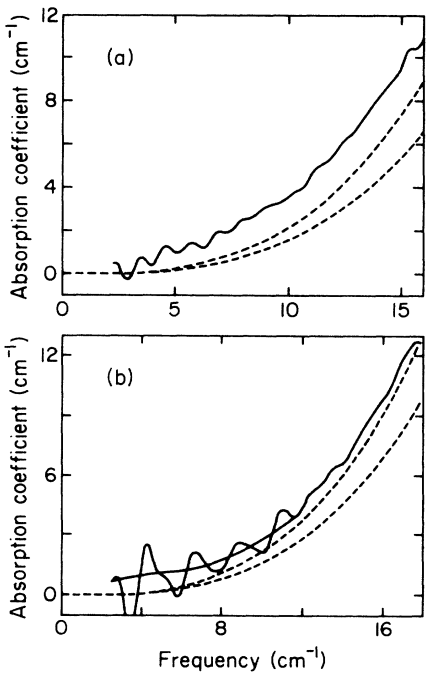

FIG. 10. Frequency dependence of the absorption coefficient of AD Ag in gelatin. (a) Material B, $f=0.142$, resolution 0.62 cm^{-1}. (b) Material C, $f=0.154$, resolutions 0.68, 2.55 cm^{-1}. The solid curves indicate the data. The dashed curves show the predictions of the Bruggeman model for 100-Å-diameter Drude Ag particles in gelatin using dielectric functions $\epsilon_h=3.3$ $+i4.73\times10^{-4}\tilde{\omega}^2$ (upper) and $\epsilon_h=3.3+i3.61\times10^{-4}\tilde{\omega}^2$ (lower) for gelatin.

dual transition to metallic behavior for increasing f in contrast with the sharp transition predicted by the BR model.

It is remarkable that any FIR radiation is transmitted through pellets of materials N and O, which are shiny in appearance and contain enough Ag to make a coin several mils thick. For pressed pellets of evaporated metal smokes mixed with alkali halides,[73] the transition to metallic behavior occurs near $f_c = 0.20$.

Figures 13–15 display the measured frequency dependence of α for samples of FD Ag-gelatin composites and the predictions of the BR model. For spectra with large interference oscillations at low frequencies, low-resolution data with reduced or no oscillations are also shown. There are two theoretical curves for each plot. The lower curve was obtained using data on FD gelatin. Since FD gelatin could not be pressed into pellets with uniform density, the prediction of α is unreliable and probably low. Thus, the prediction using "new" AD gelatin is also shown. The FD Ag-gelatin composites with low f were also difficult to press into uniform pellets. No vertical shifts were applied to the data. In general, the results show the same trends as for the AD material: Theory and experiment are in agreement for low f. With increasing f the magnitude of the measured absorption coefficient is enhanced with respect to theory, and the frequency dependence becomes weaker than cubic. α begins to diverge at a lower f, which implies greater interaction between the particles. Some agglomeration may occur during freezing. When unprotected (i.e., no gelatin) Carey Lea sol was frozen, agglomeration was apparent.

Some observations on the individual plots are in order. Figure 13 shows results for materials H-1 and F. In both cases agreement between experiment and theory is good, although the agreement can be improved by shifting the data down. The low-resolution data justify such a shift. The absorption coefficient of material E [Fig. 14(a)] is anomalous. $\alpha(\tilde{\omega})$ has a large reproducible positive zero-frequency intercept. Even a large vertical shift does not bring the data into agreement with the BR model. Material E remains a puzzle. The data for materials G, I,and J disagree with the model both in magnitude and frequency dependence. For material G, if no shift is required, the frequency dependence is sublinear. For material I, α shows a linear frequency dependence and a positive intercept. Very thin samples of material J were required to obtain transmission of FIR radiation. Thus a special technique for sample preparation was used: A pressed pellet was glued with Miller-Stephenson 907 epoxy to a LiF pellet and sanded to a thickness of 0.002 in or less. Then the LiF was wedged. The thickness of the material

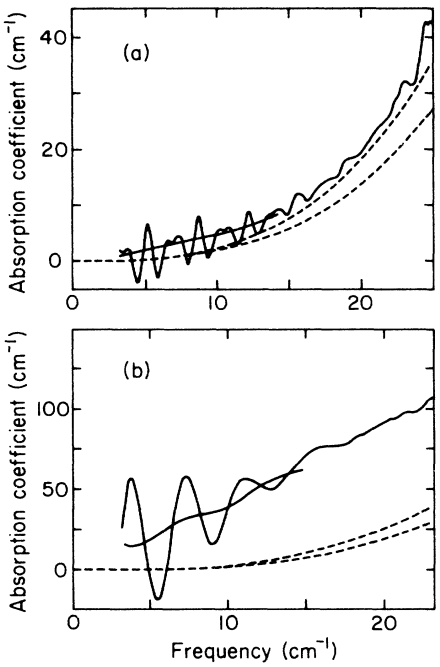

FIG. 11. Frequency dependence of the absorption coefficient of AD Ag in gelatin. (a) Material P-1, $f = 0.161$, resolution 0.47, 3.55 cm^{-1}. (b) Material P-2, $f = 0.253$, resolutions 0.90, 3.40 cm^{-1}. The solid curves indicate the data. The dashed curves show the predictions of the Bruggeman model for 100-Å-diameter Drude Ag particles in gelatin using dielectric functions $\epsilon_h = 3.3 + i4.73 \times 10^{-4}\tilde{\omega}^2$ (upper) and $\epsilon_h = 3.3 + i3.61 \times 10^{-4}\tilde{\omega}^2$ (lower) for gelatin.

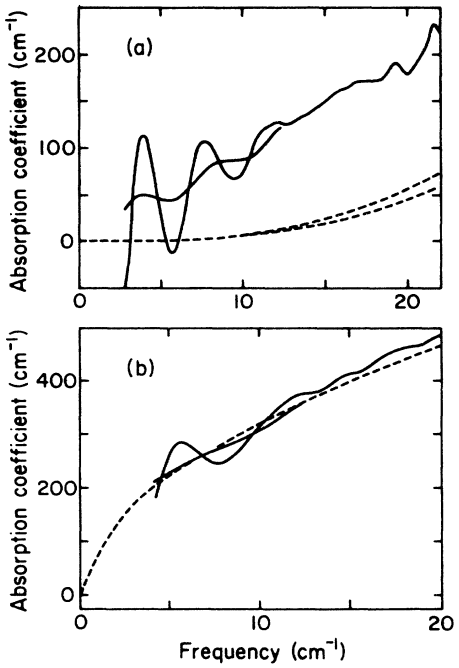

FIG. 12. Frequency dependence of the absorption coefficient of AD Ag in gelatin. The solid curves indicate high- and low-resolution data. (a) Material N, $f = 0.310$, resolutions 0.80, 3.02 cm^{-1}. The dashed curves show the predictions of the Bruggeman model for 100-Å-diameter Drude Ag particles in gelatin using dielectric functions $\epsilon_h = 3.3 + i4.73 \times 10^{-4}\tilde{\omega}^2$ (upper) and $\epsilon_h = 3.3 + i3.61 \times 10^{-4}\tilde{\omega}^2$ (lower) for gelatin. (b) Material O, $f = 0.340$, resolutions 1.28, 4.80 cm^{-1}. The dashed curve is the prediction of the Drude model using the dc conductivity $\sigma_0 = 2.25\ (\Omega\,\mathrm{cm})^{-1}$.

was neither uniform nor well known. The transmission was weak, so that α did not reproduce well from sample to sample. Therefore, results for material J are only useful as an estimate of α.

2. Volume-fraction dependence

This section discusses the dependence of the FIR absorption coefficients of the Ag-gelatin composite materials on the volume fraction of Ag. When compared with the BR model, the results for large f ($0.25 < f < 0.35$) AD material imply that the maximum possible enhancement of experiment over theory is about a factor of 10. Although the Maxwell-Garnett model is the appropriate choice by topological considerations, the BR model was used because it predicts the "percolation" behavior observed for f near $\frac{1}{3}$.

Figure 16 shows the volume-fraction dependence of α at $\tilde{\omega}=15$ cm^{-1} for the AD material. The error bars on α are standard deviations based on different combinations of pellets. The error bars on f were taken from Table I. The figure also shows the predictions of the BR model for Drude Ag in gelatin and for particles of a perfect conductor in gelatin [Eq. (11)]. In the latter case, the increase in α with f is related to absorption by the gelatin only (field exclusion mechanism). The difference between the two curves is related to absorption by the Ag particles. Thus, the BR model predicts that absorption by the particles is dominated by the gelatin absorption for $f < 0.3$. Note that the data point at $f=0.34$ lies below the prediction of the model. The fact that this material transmits radiation at all is strong evidence that the particles are well dispersed. Although the measured α for $f > 0.2$ is enhanced with respect to theory, the enhancement is never greater than about a factor of 10. There are a number of interpretations: (1) The FIR absorption by 100-Å Ag particles in a large-f composite material is anomalously enhanced, but only by an order of magnitude. (2) The BR model is incorrect for large f. An improved model would provide agreement with the data. In this interpretation the FIR absorption is not anomalous. (3) Perhaps the model is essentially correct, but there is some clustering of the particles in samples with large f. The electron micrographs for these samples are difficult to interpret.

Figure 17 shows the volume-fraction dependence of α evaluated at 18 cm^{-1} for FD Ag-gelatin composites and the predictions of the BR model. For this system, α diverges near $f=0.25$. The divergence is not as abrupt as theory predicts. The lower threshold could be due to clustering of the particles induced by the freezing process.

3. Dielectric constant

Figure 18 shows the volume-fraction dependence of the FIR dielectric constant $\bar{\epsilon}_1$ for AD Ag-gelatin composites.

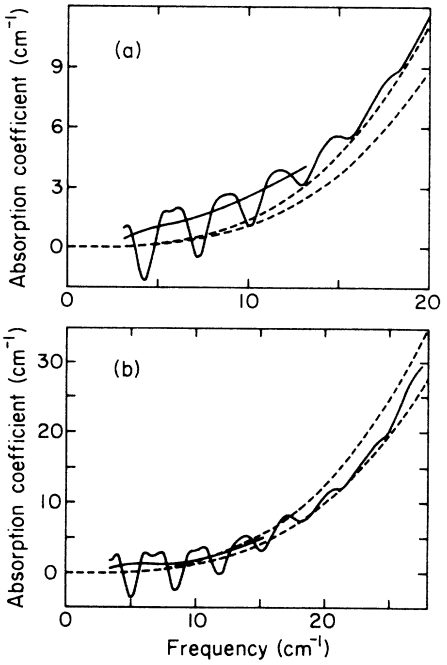

FIG. 13. Frequency dependence of the absorption coefficient of FD Ag in gelatin. The solid curves indicate high- and low-resolution data. (a) Material H-1, $f=0.062$, resolutions 0.90, 3.40 cm^{-1}. (b) Material F, $f=0.116$, resolutions 0.94, 3.55 cm^{-1}. The dashed curves show the predictions of the Bruggeman model for 100-Å-diameter Drude Ag particles in gelatin using dielectric functions $\epsilon_h = 3.3 + i3.61\times10^{-4}\tilde{\omega}^2$ (upper) and $\epsilon_h = 3.3 + i2.89\times10^{-4}\tilde{\omega}^2$ (lower) for gelatin.

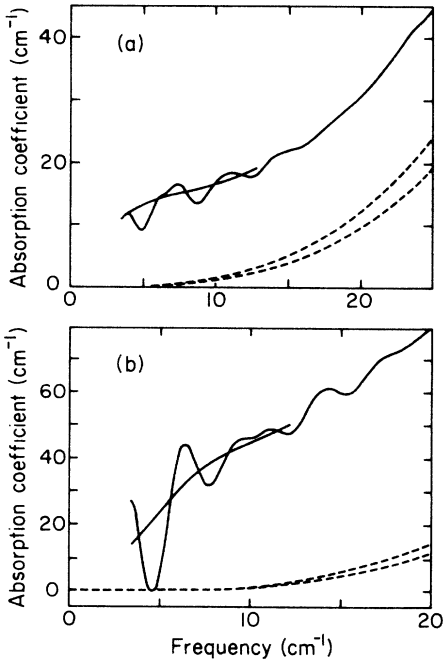

FIG. 14. Frequency dependence of the absorption coefficient of FD Ag in gelatin. The solid curves indicate high- and low-resolution data. (a) Material E, $f=0.121$, resolutions 0.94, 3.55 cm^{-1}. (b) Material G, $f=0.197$, resolutions 0.99, 3.71 cm^{-1}. The dashed curves show the predictions of the Bruggeman model for 100-Å-diameter Drude Ag particles in gelatin using dielectric functions $\epsilon_h = 3.3 + i3.61\times10^{-4}\tilde{\omega}^2$ (upper) and $\epsilon_h = 3.3 + i2.89\times10^{-4}\tilde{\omega}^2$ (lower) for gelatin.

$\bar{\epsilon}_1$ was determined for those pellets with sufficiently smooth and parallel faces that the interferograms show secondary quasi-white-light signatures due to multiple reflections. $\bar{\epsilon}_1$ increases dramatically with f in agreement with the BR model for the dc dielectric constant. Carr *et al.*[5] determined the FIR dielectric constant for Ag particles in KCl with $f<0.04$ (i.e., small f) and also found agreement with effective-medium theories.

4. *Temperature and magnetic field dependences*

No dependence of the FIR absorption coefficient of the Ag-gelatin composite on either temperature or magnetic field was observed. Specifically, any temperature or field dependence is buried in the noise and hence must certainly be less than 1% of the total absorption over the range covered. A sample of acetone-dried material N was studied at $T\simeq 1$ K with $H=0$ and 60 kG, and for a number of temperatures up to 23 K at $H=0$. The absorption by samples of material C and AD gelatin without Ag particles also showed no dependence on T or H. No search was made for magnetic field dependence in the FD material. No frequency-dependent change was observed in the absorption for materials I and J when the ^{4}He bath in which the samples were immersed was pumped.

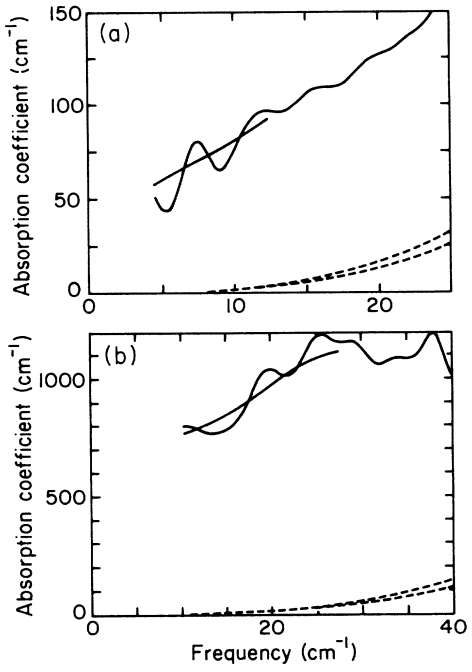

FIG. 15. Frequency dependence of the absorption coefficient of FD Ag in gelatin. The solid curves indicate high- and low-resolution data. (a) Material I, $f=0.219$, resolutions 1.28, 4.80 cm^{-1}. (b) Material J, $f=0.244$, resolutions 2.71, 10.2 cm^{-1}. The dashed curves show the predictions of the Bruggeman model for 100-Å-diameter Drude Ag particles in gelatin using dielectric functions $\epsilon_h=3.3+i3.61\times10^{-4}\tilde{\omega}^2$ (upper) and $\epsilon_h=3.3+i2.89\times10^{-4}\tilde{\omega}^2$ (lower) for gelatin.

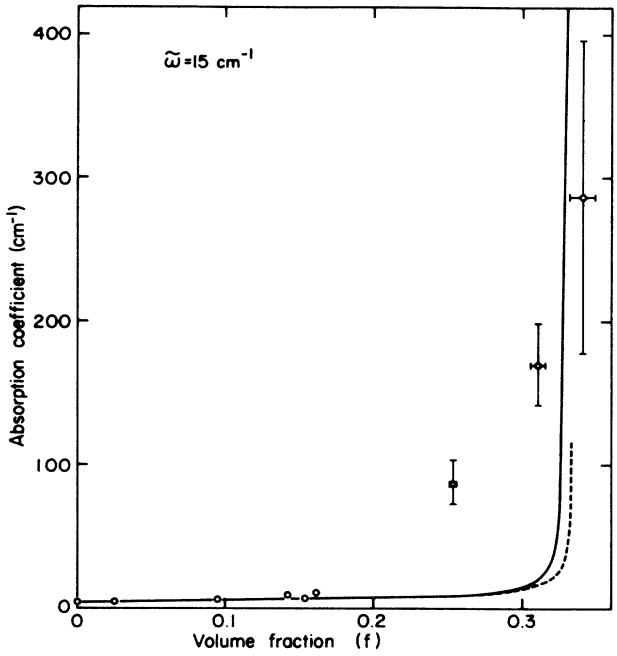

FIG. 16. Volume-fraction dependence of the absorption coefficient at $\tilde{\omega}=15$ cm^{-1} for AD Ag in gelatin. Circles indicate the data. The solid line shows the prediction of the Bruggeman model for 100-Å-diameter Drude Ag particles imbedded in gelatin with dielectric function $\epsilon_h=3.3+i3.61\times10^{-4}\tilde{\omega}^2$. The dashed curve represents the BR model for particles made up of a perfect conductor.

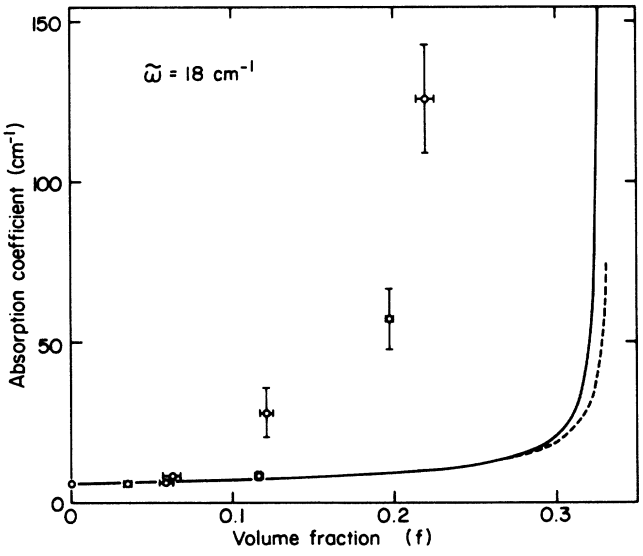

FIG. 17. Volume-fraction dependence of the absorption coefficient at $\tilde{\omega}=18$ cm^{-1} for FD Ag-gelatin composite. Circles indicate the data. The solid line shows the prediction of the Bruggeman model for 100-Å-diameter Drude Ag particles imbedded in gelatin with dielectric function $\epsilon_h=3.3+i2.89\times10^{-4}\tilde{\omega}^2$. The dashed curve represents the BR model for particles made up of a perfect conductor.

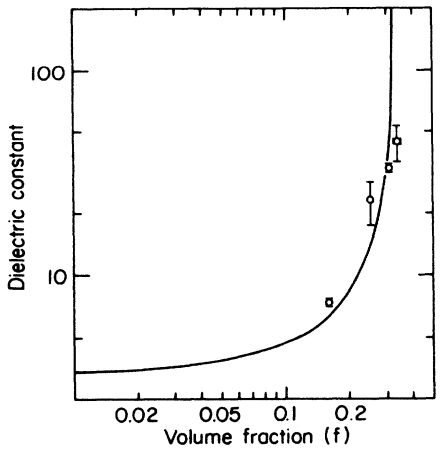

FIG. 18. Volume-fraction dependence of the FIR dielectric constant of AD Ag-gelatin composite. Circles indicate the data. The solid line represents the dc dielectric constant predicted by the Bruggeman model: $\bar{\epsilon}_1 = 3.3/(1-3f)$.

C. Far-infrared absorption by agglomerated particles

This section discusses FIR absorption by Ag-gelatin composites for which the Ag particles were deliberately clumped during preparation. The samples under consideration have only a few percent of Ag by volume.

Figure 19 shows α/f, measured at $\tilde{\omega}=23$ cm^{-1}, versus the volume of 400 g/l sodium-citrate solution added to 37 ml of Carey Lea sol. The results for the K and L series, which were prepared from separate batches of sol, are consistent. The error bars take into account the error in f (Table I) and the standard deviation of α based on different combinations of pellets. The scatter in the points at low citrate concentration, which is larger than the error bars, might be due to difficulty in pressing uniform pellets. The absorption per particle increases dramatically as sodium citrate is added to induce clumping. Samples with the most agglomeration, i.e., those to which the largest quantity of sodium citrate was added, show enhanced absorption of the same magnitude as observed for pressed pellets of Ag in KCl.[5] This effect is remarkable because the absorption coefficient of Drude Ag particles is dominated by the gelatin by about 3 orders of magnitude.

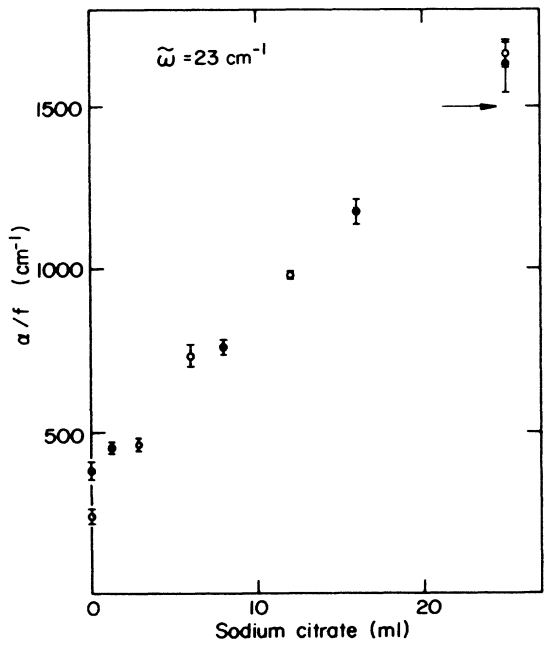

FIG. 19. Absorption coefficient at $\tilde{\omega}=23$ cm^{-1}, normalized by the volume fraction of Ag, vs volume of sodium-citrate solution added to induce agglomeration of the particles for FD Ag-gelatin composite. The open and solid circles represent data on the K and L series of materials, respectively. The arrow indicates α/f for pressed pellets of Ag particles in KCl taken from Fig. 3 of Carr *et al.*[5]

One might argue that the enhanced absorption is induced by the sodium citrate and has nothing to do with the Ag particles. Figure 20 shows α ($\tilde{\omega}=23$ cm^{-1}) for the entire L series, which includes samples prepared without Ag particles. Although addition of sodium citrate to gelatin increases the absorption slightly, the effect is much larger when Ag particles are present. For the samples without Ag, it is surprising that α rises at all. Sodium citrate has a lower absorption coefficient than gelatin at 23 cm^{-1}, and its dielectric constant is not sufficiently large to produce the enhancement described in Sec. II B. The absorption coefficient at low sodium-citrate concentration might be artificially reduced due to difficulty in compressing the material into uniform pellets. Material with lots of sodium citrate in it was easier to handle. The absorption coefficient of the Ag-gelatin composite falls off for large concentrations of sodium citrate because the volume fraction of Ag is smaller.

Figure 21 shows α/f at $\tilde{\omega}=23$ cm^{-1} for the M series, for which a second agent, sodium nitrate, was used to induce clumping. The volumes of $1M$ $NaNO_3$ indicated on the abscissa were added to 37-ml portions of Carey Lea

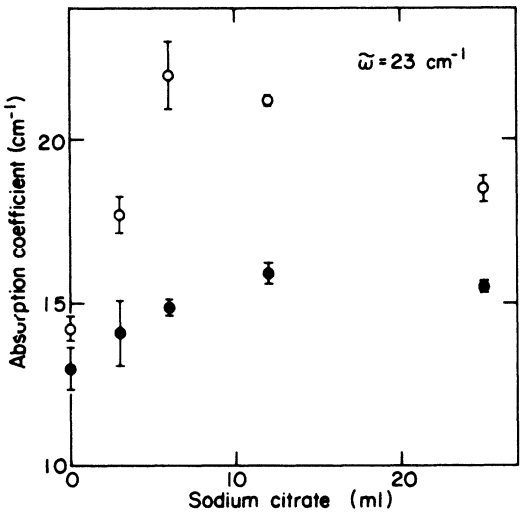

FIG. 20. Absorption coefficient at $\tilde{\omega}=23$ cm^{-1} vs volume of added sodium-citrate solution for the L series of FD materials. Open circles represent materials that contain Ag particles. Solid circles represent samples containing gelatin and sodium citrate only.

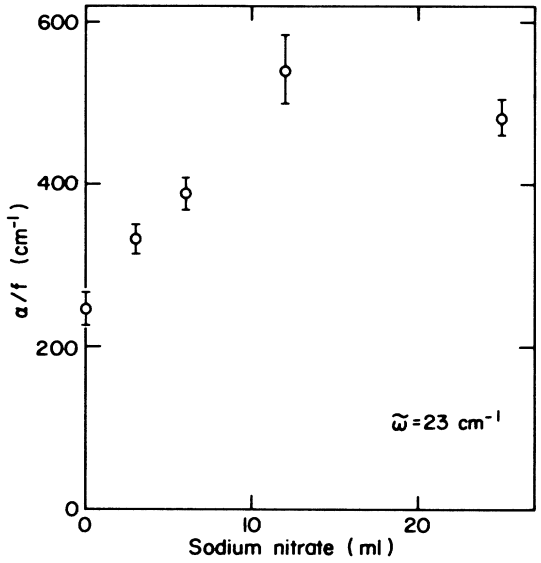

FIG. 21. Absorption coefficient at $\tilde{\omega}=23$ cm^{-1} normalized by the volume fraction of Ag vs volume of $NaNO_3$ solution added to induce agglomeration of the particles for FD Ag in gelatin. Data on the *M* series of materials are shown.

sol. Increased absorption with added $NaNO_3$ is observed, but the effect is smaller than for sodium citrate. $NaNO_3$ in gelatin without Ag particles is a weaker absorber than the corresponding sample with Ag.

V. DISCUSSION

The FIR data on well-dispersed particles can be used to place bounds on the magnitude of the enhancement of the measured absorption coefficient over theory that are 2 orders of magnitude lower than the enhancements reported for metal smokes imbedded in alkali halides. The results for AD material are chosen because the particles are apparently better dispersed. The data begin to diverge from the prediction of the BR model near $f=0.15$. Since absorption by the Ag particles is just becoming observable, the results near $f=0.15$ will be used to place a bound. Because absorption by the gelatin dominates for the low-f samples, one does not know α for the particles. Thus, the results for $f<0.15$ are also consistent with no enhancement whatsoever.

The first argument for an upper bound on single-particle absorption is based on Fig. 22. Although absorption by the particles and gelatin do not simply add, the figure shows a naive estimate of α/f for the Ag particles in material *C* obtained by subtracting the gelatin absorption from the measured absorption before normalizing by f. The absorption spectrum for material *C* has been shifted by 0.7 cm^{-1} so that α vanishes at zero frequency. The gelatin absorption is that of "old" AD gelatin, which is appropriate for material *C*. For clarity, the figure does not show the oscillations due to interference, but the data at lower frequencies should be regarded as more uncertain. Note that the BR model provides excellent agreement with the measured absorption coefficient of material *C* when the dielectric functions of "old" AD gelatin and Drude Ag are used. Figure 22 also shows the prediction

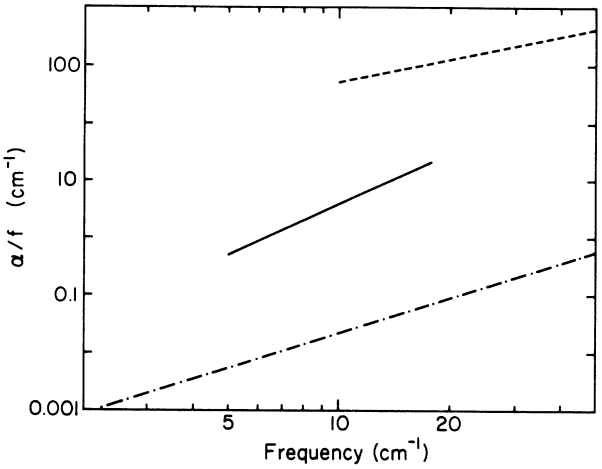

FIG. 22. Frequency dependence of the absorption coefficient normalized by the volume fraction of Ag. The dashed line represents data on a pressed pellet of Ag particles in KCl taken from Fig. 3 of Carr *et al.*[5] The dashed-dotted line shows the prediction of the Bruggeman model for 100-Å-diameter Drude Ag particles in KCl. Experiment and theory disagree by a factor of about 10^4. The solid line is an estimate of absorption by Ag particles in gelatin obtained by subtraction of the gelatin absorption from the Ag-gelatin absorption for material *C*. The disagreement with theory is a factor of 100.

of the BR model for 100-Å-diameter particles of Drude Ag in nonabsorbing KCl ($\epsilon_0=4.64$) and the corresponding experimental result.[5] Unfortunately, Carr *et al.*[5] did not specify the size of the Ag particles used in their Fig. 3. The experimental result for Ag in KCl is enhanced by 4 orders of magnitude over theory. The figure indicates that the maximum possible enhancement of absorption by well-dispersed Ag in gelatin is a factor of 100.

Another way to place a bound on the possible enhancement is to determine the factor by which a parameter of Drude Ag must be modified to produce a noticeable change in the prediction of the BR model for α. The relaxation time τ is an appropriate parameter, since the electric dipole term of the absorption coefficient for isolated small Drude metal particles imbedded in a nonabsorbing dielectric is proportional to $1/\tau$. Figure 23 shows the absorption coefficient for material *C* and the absorption predicted by the BR model for Drude Ag particles with adjustable τ in "old" AD gelatin. The measured α has been downshifted by 0.7 cm^{-1}. τ must be decreased by a factor of 100 to obtain a significant disagreement between theory and experiment. Thus, this argument also leads to the conclusion that the maximum possible enhancement is about 2 orders of magnitude. The data for $f=0.15$ material are also consistent with the BR model if there is no enhancement whatsoever.

Burtscher and Schmidt-Ott[74] have reported an enhancement of at least 10^4 in the dispersion (van der Waals) forces between Ag particles in aerosols. Since the dispersion force is proportional to the polarizability, the polarizability should also be enhanced by 10^4. The FIR data on Ag particles in gelatin are inconsistent with such a large enhancement.

Recent theoretical work demonstrates that clustered

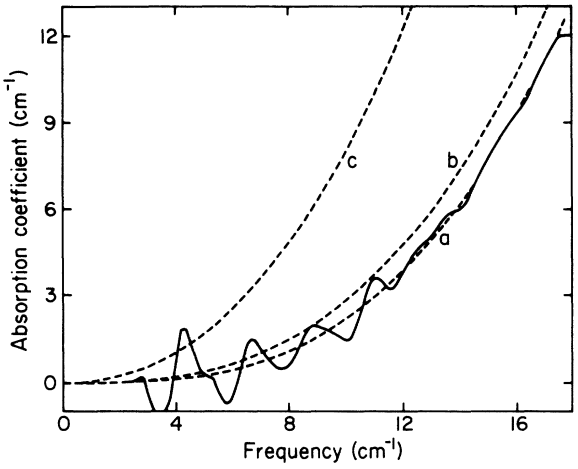

FIG. 23. Estimate of the maximum enhancement of the absorption by $x=100$-Å-diameter Drude Ag particles consistent with the data on acetone-dried Ag gelatin (material C). The solid curve shows the data. The dashed curves are the predictions of the Bruggeman model with $\hbar\omega_p=9.0$ eV and (a) $\tau=\tau_0$, (b) $\tau=\tau_0\times10^{-2}$, and (c) $\tau=\tau_0\times10^{-3}$, where $\tau_0=2x/v_F$ and $v_F=1.38\times10^8$ m/s. τ must be modified by a factor of 10^2 to obtain a significant disagreement.

particles show enhanced electric dipole absorption.[21–24] Here the simple clustering model introduced in Sec. II C is applied to the Ag-gelatin composite. First, consider the enhancement predicted by the model in the absence of absorption by the gelatin host. Figure 24 shows the calculated absorption by Ag particles in nonabsorbing gelatin ($\epsilon_h=3.3$). The clustering model predicts an enhancement by a factor of 20 over the BR model (electric dipole term only), which describes a well-dispersed system. This enhancement is relatively small compared to enhancements predicted by other clustering calculations applied to the FIR.[21,22,24]

Figure 25 shows the absorption coefficient for $f=0.05$ Ag-gelatin composite predicted by the BR model and the

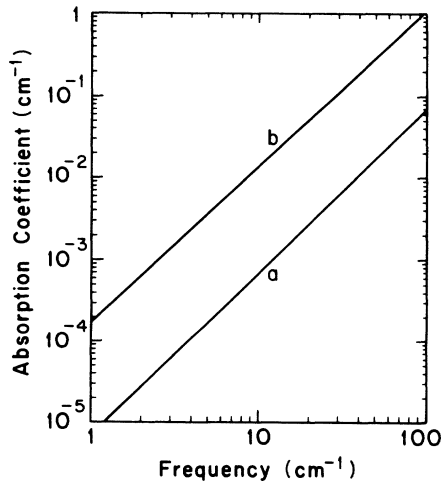

FIG. 24. Calculated absorption coefficient for Drude Ag particles in nonabsorbing gelatin ($\epsilon_h=3.3$). $f=0.05$. (a) Bruggeman model, (b) clustering model.

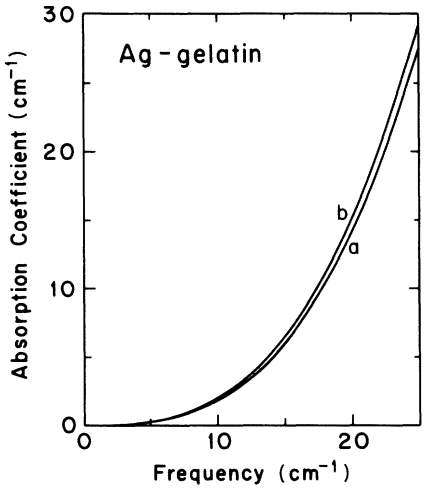

FIG. 25. Calculated absorption coefficient for Drude Ag particles in gelatin. $\epsilon_h=3.3+i4.73\times10^{-4}\tilde{\omega}^2$ for gelatin and $f=0.05$. (a) Bruggeman model, (b) clustering model.

clustering model. Although absorption by the Ag particles is dominated by gelatin absorption, an enhancement of about 6% is observed in the absorption by clusters. Since the BR model provides a good description of the data for low f, clustering is not important in these samples.

An important feature of this work is the broad range of metallic volume fractions under consideration. Most work in the FIR has focussed on samples with low f. Although the BR model agrees with our data at low f, it is not successful for large f. The transition to large absorption as the percolation threshold is approached is much broader in the data than predicted by theory. Mean-field theories such as the BR model are not expected to strictly apply near the percolation threshold.[75] Further theoretical work is required to explain the data.

VI. CONCLUSIONS

A detailed experimental study of far-infrared absorption of Ag particles imbedded in gelatin has been performed. Analysis of the results leads to several conclusions regarding the "anomalous FIR absorption" and the applicability of standard effective-medium theories to the FIR properties of composite materials. First, no evidence for anomalously enhanced absorption was observed in low-f samples containing well-dispersed particles. The lack of observable absorption by the particles for $f<0.15$ leads to bounds on its magnitude, using the data near $f=0.15$. These bounds do not exclude the possibility of enhanced absorption by isolated Ag particles. The arguments presented here are subtle because gelatin absorbs FIR radiation. Second, samples containing deliberately agglomerated particles show enhanced absorption. Thus, clustering of the particles is convincingly associated with enhanced absorption in this Ag-gelatin composite. Finally, the Bruggeman model does not provide an adequate description of FIR absorption by the Ag-gelatin composite when the concentration of Ag particles is large ($f>0.15$). Further theoretical work is required to under-

stand in detail the FIR properties of composite materials, particularly near the dc percolation threshold. Additional experiments on composite materials covering a broad range of composition are also required to determine whether the results presented here are general or unique to Ag-gelatin composites.

ACKNOWLEDGMENTS

We thank John Telford for helpful discussions on sample preparation and for performing the ultramicrotomy. Ray Coles, John Hunt, and Margaret Kraft are thanked for assistance on the electron microscopes. Ronnie Spitzer performed the resistivity measurements. We thank Ralph Sherriff for comments on the manuscript. This work was supported at Cornell University by the National Science Foundation under Grant No. DMR-87-14600 and the U.S. Army Research Office Contract No. DAAL03-86-K-0103 and at the University of Pittsburgh by the Office of Naval Research, U.S. Department of Defense, Contract No. N00014-85-K-0808.

[1]D. B. Tanner, A. J. Sievers, and R. A. Buhrman, Phys. Rev. B **11**, 1330 (1975).
[2]C. G. Granqvist, R. A. Buhrman, J. Wyns, and A. J. Sievers, Phys. Rev. Lett. **37**, 625 (1976).
[3]D. P. Pramanik, M. S. thesis, Cornell University (1978).
[4]N. E. Russell, J. C. Garland, and D. B. Tanner, Phys. Rev. B **23**, 632 (1981).
[5]G. L. Carr, R. L. Henry, N. E. Russell, J. C. Garland, and D. B. Tanner, Phys. Rev. B **24**, 777 (1981).
[6]A. J. Glick and E. D. Yorke, Phys. Rev. B **18**, 2490 (1978).
[7]E. Simanek, Solid State Commun. **37**, 97 (1981).
[8]H. J. Trodahl, Phys. Rev. B **19**, 1316 (1979); J. Phys. C **15**, 7245 (1982).
[9]A. G. Mal'shukov, Zh. Eksp. Teor. Fiz. **85**, 700 (1983) [Sov. Phys.—JETP **58**, 409 (1983)].
[10]P. Apell, Phys. Scr. **29**, 146 (1984).
[11]P. Chylek, D. Boice, and R. G. Pinnick, Phys. Rev. B **27**, 5107 (1983). See also D. B. Tanner, *ibid.* **30**, 1042 (1984); P. Chylek and V. Srivastava, *ibid.* **30**, 1008 (1984).
[12]A. A. Lushnikov, V. V. Maksimenko, and A. J. Simonov, in *Electromagnetic Surface Modes,* edited by J. Boardman (Wiley, New York, 1982), Ch. 8; Fiz. Tverd. Tela (Leningrad) **20**, 505 (1978) [Sov. Phys.—Solid State **20**, 292 (1978)]; V. V. Maksimenko, A. J. Simonov, and A. A. Lushnikov, Phys. Status Solidi B **83**, 377 (1977); A. A. Lushnikov and A. J. Simonov, Phys. Lett. **44A**, 45 (1973).
[13]C. G. Granqvist, Z. Phys. B **30**, 29 (1978).
[14]E. Simanek, Phys. Rev. Lett. **38**, 1161 (1977).
[15]R. Ruppin, Phys. Rev. B **19**, 1318 (1977).
[16]P. N. Sen and D. B. Tanner, Phys. Rev. B **26**, 3582 (1985).
[17]C. G. Granqvist and R. A. Buhrman, J. Appl. Phys. **47**, 2200 (1976).
[18]R. P. Devaty and A. J. Sievers, Phys. Rev. Lett. **52**, 1344 (1984).
[19]W. A. Curtin, R. C. Spitzer, N. W. Ashcroft, and A. J. Sievers, Phys. Rev. Lett. **54**, 1071 (1985).
[20]S.-I. Lee, T. W. Noh, K. Cummings, and J. R. Gaines, Phys. Rev. Lett. **55**, 1626 (1985).
[21]W. A. Curtin and N. W. Ashcroft, Phys. Rev. B **31**, 3287 (1985).
[22]P. M. Hui and D. Stroud, Phys. Rev. B **33**, 2163 (1986).
[23]G. A. Niklasson, S. Yatsuya, and C. G. Granqvist, Solid State Commun. **59**, 579 (1986).
[24]F. Claro and R. Fuchs, Phys. Rev. B **33**, 7956 (1986).
[25]R. Monreal, J. Giraldo, F. Flores, and P. Apell, Solid State Commun. **54**, 661 (1985).
[26]X. M. Hua and J. I. Gersten, Phys. Rev. B **31**, 855 (1985).
[27]P. de Andres, R. Monreal, and F. Flores, Phys. Rev. B **34**, 2886 (1986).
[28]P. de Andres, R. Monreal, and F. Flores, Phys. Rev. B **34**, 7365 (1986).
[29]R. Monreal, P. de Andres, and F. Flores, J. Phys. C **18**, 4951 (1985).
[30]T. W. Noh, S.-I. Lee, and J. R. Gaines, Phys. Rev. B **33**, 1401 (1986); T. W. Noh, S.-I. Lee, Y. Song, and J. R. Gaines, Phys. Rev. B **34**, 2882 (1986).
[31]S.-I. Lee, T. W. Noh, and J. R. Gaines, Phys. Rev. B **32**, 3580 (1985); S.-I. Lee, T. W. Noh, J. Golben, and J. R. Gaines, Phys. Rev. B **33**, 5844 (1986).
[32]Y. H. Kim and D. B. Tanner, Phys. Rev. B **39**, 3585 (1989).
[33]G. L. Carr, S. Perkowitz, and D. B. Tanner, in *Infrared and Millimeter Waves,* edited by K. J. Button (Academic, Orlando, 1984), Vol. 15.
[34]W. P. Halperin, Rev. Mod. Phys. **58**, 533 (1986).
[35]J. A. A. J. Perenboom, P. Wyder, and F. Meier, Phys. Rep. **78**, 173 (1981).
[36]H. P. Baltes and E. Simanek, in *Aerosol Microphysics II,* Vol. 29 of *Topics in Current Physics,* edited by W. H. Marlow (Springer-Verlag, Berlin, 1982), p. 7.
[37]R. P. Devaty, Physica A **157**, 262 (1989).
[38]D. A. G. Bruggeman, Ann. Phys. (Leipzig) [Folge 5] **24**, 636 (1935).
[39]D. M. Wood and N. W. Ashcroft, Philos. Mag. **35**, 269 (1977).
[40]R. Landauer, in *Electrical Transport and Optical Properties of Inhomogeneous Media, Ohio State University, 1977,* Proceedings of the First Conference on the Electrical Transport and Optical Properties of Inhomogeneous Media, AIP Conf. Proc. **40**, edited by J. C. Garland and D. B. Tanner (AIP, New York, 1978), p. 2.
[41]W. Lamb, D. M. Wood, and N. W. Ashcroft, Phys. Rev. B **21**, 2248 (1980).
[42]J. C. M. Garnett, Philos. Trans. R. Soc. London **203**, 385 (1904); **205**, 237 (1906).
[43]D. Stroud and F. P. Pan, Phys. Rev. B **17**, 1602 (1978).
[44]J. D. Jackson, *Classical Electrodynamics,* 2nd ed. (Wiley, New York, 1975), pp. 197, 198.
[45]L. D. Landau and E. M. Lifshitz, *Electrodynamics of Continuous Media* (Pergamon, New York, 1975), p. 193.
[46]G. Mie, Ann. Phys. **25**, 377 (1908). See also M. Born and E. Wolf, *Principles of Optics,* 5th ed. (Pergamon, New York, 1975), p. 635 ff.
[47]J. Euler, Z. Phys. **137**, 318 (1954); W. T. Doyle, Phys. Rev. **111**, 1067 (1958); U. Kreibig, J. Phys. F **4**, 999 (1974).
[48]N. W. Ashcroft and N. D. Mermin, *Solid State Physics* (Holt, Rinehart and Winston, New York, 1976), p. 5, Appendix A.
[49]M. Carey Lea, Am. J. Sci. **37**, 476 (1889).
[50]M. Kerker, O. Siiman, L. A. Bumm, and D.-S. Wang, Appl. Opt. **19**, 3253 (1980).

[51]G. Frens and J. Th. G. Overbeek, Kolloid Z. Z. Polym. **233**, 922 (1969).
[52]M. Mabuchi, T. Takenaka, Y. Fujiyoshi, and N. Uyeda, Surf. Sci. **119**, 150 (1982).
[53]W. J. Miller and A. H. Herz, in *Colloid and Interface Science, Vol. IV. Hydrosols and Rheology,* edited by M. Kerker (Academic, New York, 1976), pp. 315–329.
[54]For example, see U. Kreibig, Z. Phys. B **31**, 39 (1978).
[55]M. A. Hayat, *Principles and Techniques of Electron Microscopy* (Van Nostrand Reinhold, New York, 1972), Vol. 1.
[56]C. Kittel, *Introduction to Solid State Physics,* 4th ed. (Wiley, New York, 1971), p. 39.
[57]R. P. Devaty, Ph.D. thesis, Cornell University, 1983.
[58]H. H. Willard, L. L. Merritt, J. A. Dean, and F. A. Settle, *Instrumental Methods of Analysis,* 6th ed. (Wadsworth, Belmont, CA, 1981), Ch. 21.
[59]D. A. Skoog and D. M. West, *Fundamentals of Analytical Chemistry,* 3rd ed. (Saunders College, Philadelphia, 1976), Ch. 24.
[60]H. A. Strobel, *Chemical Instrumentation: A Systematic Approach,* 2nd ed. (Addison-Wesley, Reading, MA, 1973), Chap. 24.
[61]*CRC Handbook of Chemistry and Physics,* 66th ed., edited by R. C. Weast (CRC, Boca Raton, FL, 1982), p. B222.
[62]C. W. Mays, J. S. Vermaak, and D. Kuhlmann-Wilsdorf, Surf. Sci. **12**, 134 (1968).
[63]E. F. Fullam, Rev. Sci. Inst. **43**, 245 (1972).
[64]Ph. Buffat and J.-P. Borel, Phys. Rev. A **13**, 2287 (1976).
[65]C. J. Coombes, J. Phys. F **2**, 441 (1972).
[66]I. G. Nolt, R. D. Kirby, C. D. Lytle, and A. J. Sievers, Appl. Opt. **8**, 309 (1969); I. G. Nolt, Ph.D. thesis, Cornell University, 1967.
[67]D. B. Tanner, Ph.D. thesis, Cornell University, 1972.
[68]H. D. Drew and A. J. Sievers, Appl. Opt. **8**, 2067 (1969); H. D. Drew, Ph.D. thesis, Cornell University, 1968.
[69]K. K. Mon and A. J. Sievers, Appl. Opt. **14**, 1054 (1975).
[70]R. L. Blewitt and A. J. Sievers, J. Low Temp. Phys. **13**, 617 (1973).
[71]M. Born and E. Wolf, *Principles of Optics,* 5th ed. (Pergamon, New York, 1975), pp. 628–632; O. S. Heavens, *Optical Properties of Thin Solid Films* (Academic, New York, 1955), pp. 59–62; P. C. Taylor, U. Strom, J. R. Hendrickson, and S. K. Behl, Phys. Rev. B **13**, 1711 (1976). Note that Eq. (1) in Ref. 4 is missing some factors.
[72]F. E. Pinkerton, Ph.D. thesis, Cornell University, 1981.
[73]D. M. Grannan, J. C. Garland, and D. B. Tanner, Phys. Rev. Lett. **46**, 375 (1981).
[74]H. Burtscher and A. Schmidt-Ott, Phys. Rev. Lett. **48**, 1734 (1982).
[75]Y. Yagil and G. Deutscher, Appl. Phys. Lett. **52**, 374 (1988), and references therein.

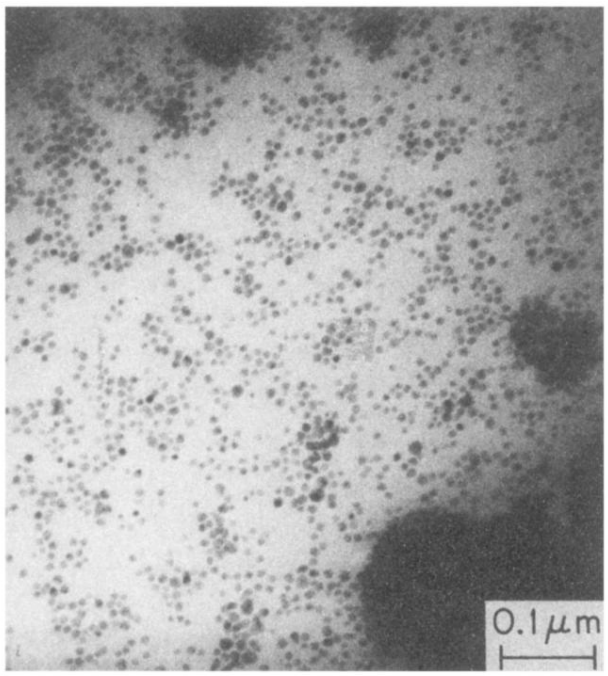

FIG. 3. Transmission electron micrograph of dried Carey Lea sol taken with the JEM 200.

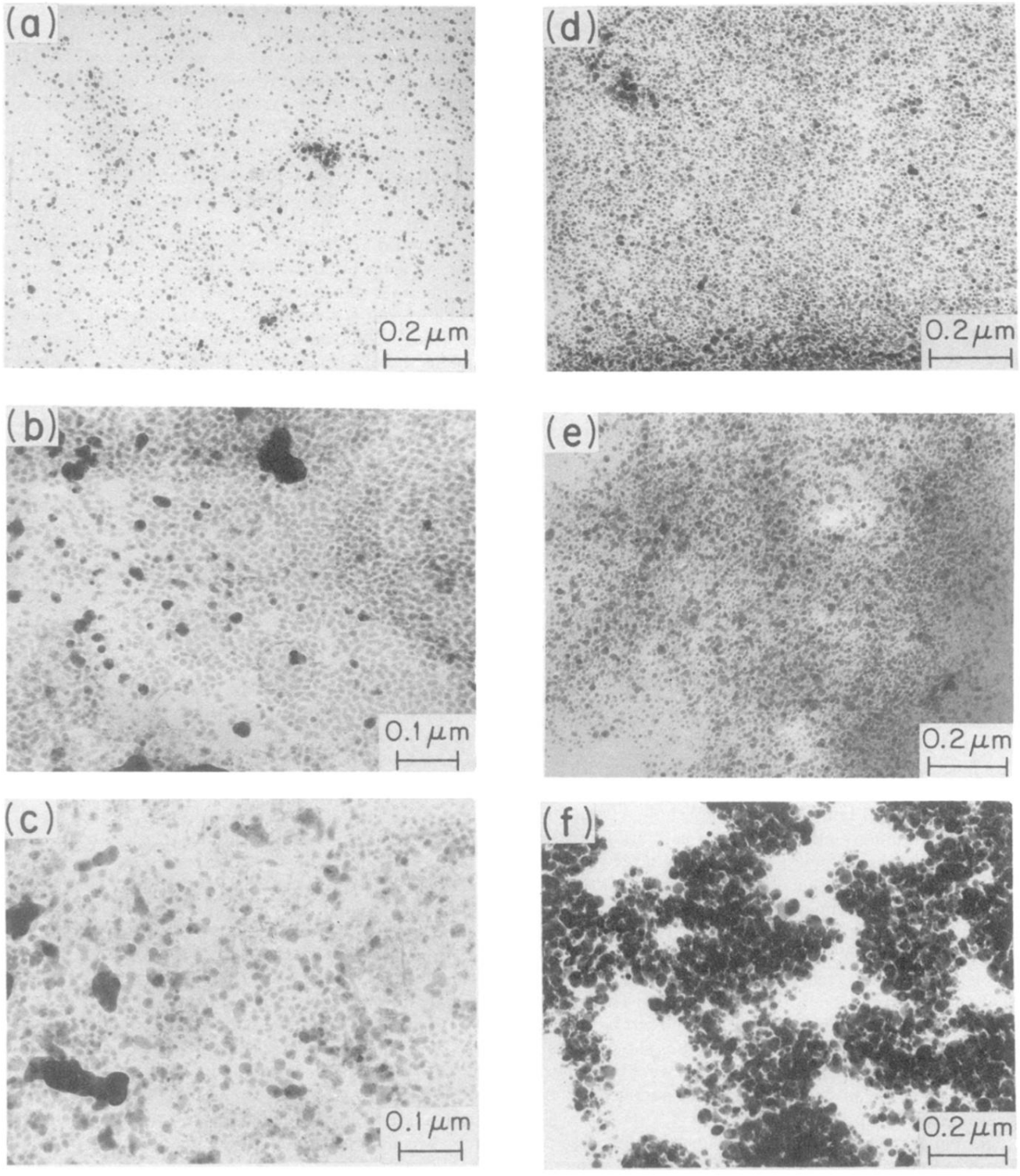

FIG. 4. Transmission electron micrographs of Ag imbedded in gelatin: (a) Material *A*, (b) *P*-1, (c) *O*, (d) *H*-1, (e) *F*, (f) *J*. (a)–(c) shows AD material, (d)–(f) FD. The lower micrographs correspond to higher f. Micrographs (b) and (c) were taken with the JEOL 200CX, the remainder with the JEM 200.